

A platform for functionalization of cellulose, chitin/chitosan, alginate with polydopamine: A review on fundamentals and technical applications

Peer-reviewed author version

SAMYN, Pieter (2021) A platform for functionalization of cellulose, chitin/chitosan, alginate with polydopamine: A review on fundamentals and technical applications. In: International journal of biological macromolecules, 178 , p. 71 -93.

DOI: 10.1016/j.ijbiomac.2021.02.091

Handle: <http://hdl.handle.net/1942/35413>

**A Platform for Functionalization of Cellulose, Chitin/chitosan, Alginate with Polydopamine:
A Review on Fundamentals and Technical Applications.**

Pieter Samyn*

Hasselt University, Institute for Materials Research, Applied and Analytical Chemistry,
Agoralaan Gebouw D, B-3590 Diepenbeek, tel. +32 11 26 85 94

*Contact: pieter.samyn@outlook.be

ABSTRACT

Nature provides concepts and materials with interesting functionalities to be implemented in innovative and sustainable materials. In this review, it is illustrated how the combination of biological macromolecules, i.e. polydopamine and polysaccharides (cellulose, chitin/chitosan, alginate), enables to create functional materials with controlled properties. The mussel-adhesive properties rely on the secretion of proteins having 3,4-dihydroxyphenylalanine amino acid with catechol groups. Fundamental understanding on the biological functionality and interaction mechanisms of dopamine in the mussel foot plaque is presented in parallel with the development of synthetic analogues through extraction or chemical polymer synthesis. Subsequently, modification of cellulose, chitin or alginate and their nanoscale structures with polydopamine is discussed for various technical applications, including bio- and nanocomposites, films, filtration or medical membranes, adhesives, aerogels, or hydrogels. The presence of polydopamine stretches far beyond surface adhesive properties, as it can be used as an intermediate to provide additional performance of hydrophobicity, self-healing, antimicrobial, photocatalytic, sensoric, adsorption, biocompatibility, conductivity, coloring or mechanical reinforcement. The dopamine-based ‘green’ chemistry can be extended towards generalized catechol chemistry for modification of polysaccharides with tannic acid, caffeic acid or laccase-mediated catechol functionalization. Therefore, the modification of polysaccharides with polydopamine or catechol analogues provides a general platform for sustainable material functionalization.

Keywords: cellulose, nanocellulose, chitin, alginate, polydopamine, catechol

1. INTRODUCTION

The in-depth study of materials in surrounding nature is a great source of inspiration for the design of innovative technical and sustainable applications. In recent decades, bio-mimicry developed as an attractive scientific discipline for creating novel technologies, fabrication methods, smart materials and/or surfaces with novel functionalities. The re-thinking of full design concepts may lead to processes with lower environmental footprint due to, e.g., reduced toxicity, lower amounts of harsh chemical treatments, reduction in number of processing steps, smoother processing conditions under low temperature and aqueous conditions, replacement of oil-based into bio-based polymers and many more. However, it needs an interdisciplinary approach between biologists, chemists and materials engineers with thorough understanding of fundamental functionalities of the candidate-biomolecules in its native environment in order to make a correct translation into efficient technological applications.

The mechanisms for bio-adhesion are based on the secretion of specific chemical substances [1], the creation of unique surface textures [2], and/or a combination of both [3]. Many bio-adhesives are specifically adapted to a given environment, such as dry conditions [4], wet conditions [5], underwater conditions under specific pH [6], and they can be reversible or permanent [7]. The dry adhesion relies on van der Waals forces executed near multiple contact elements, which are formed by multiscale fibrillar filaments at the surface of, e.g., insects or gecko feet [8]. The wet adhesion is established through capillary forces that allow for the drainage of liquids and hence increase in friction [9]. The secretion of adhesive components such as proteins [10], or polysaccharides [11], contributes to chemical adhesion in plants or molluscs (e.g., barnacles, mussels, sandcastle worms). The development of synthetic analogues for bio-adhesives requires extensive research at a macromolecular level including different stages, *(i)* to understand molecular and mechano-chemical aspects controlling both adhesive and cohesive interactions in bio-adhesive systems, *(ii)* to select functional adhesive species/groups, and *(iii)* to synthesize and optimize molecular composition and crosslinking conditions of equivalent materials [12]. The bio-adhesives may be elegantly transferred into technical applications [13]: besides the creation of novel bio-based bulk adhesives, it particularly allows for the design of new adhesive interface concepts [14]. The creation of bio-adhesive surfaces, coatings and interfaces stretches beyond the aim to purely provide good mechanical adhesion under most difficult circumstances (e.g., non-polar surfaces, water environment), but it also aims to develop additional surface functionalities, such as water resistance, hydrophobicity, anti-corrosion, wettability, lubrication, self-healing properties, self-cleaning effect, controlled release, biocompatibility, anti-microbial activity, electrical conductivity [15]. Indeed, various examples of adequate surface design, topography and patterns are offered by nature to comply with many of those challenging requirements. The high interest in bio-adhesive materials specifically raised in recent decades to oppose environmental concerns about resource depletion, hazardous chemicals, emission of organic volatiles from solvents, biodegradability, or recyclability.

The polysaccharides are abundantly available biopolymers with versatile structures and various morphological, chemical and physical properties. In this review, the cellulose, chitin/chitosan and alginate polysaccharides are particularly addressed. Due to the excellent mechanical properties, they can be used as a substrate, additive or matrix element, while their good reactivity allows to introduce additional functionalities. In nature, the self-adhesion of cellulose and its nanoscale components has been recognized through a high density of hydroxyl groups at the fiber or fibril surface [16], and its adhesion in wood matrices is controlled by the presence of hemicellulose as an interface compatibilizer [17]. For chitin/chitosan polysaccharides, electrostatic charges at surfaces provide them with evidence for adhesion in barnacles [18]. The formation of complexes between chitin and proteins was observed in many natural materials [19]. The interaction between chitin microfibrils and proteins during the cell wall synthesis of fungi happens through interface charges and the intimate layered structures result in high mechanical strength [20]. The other anionic polysaccharides such as alginates are present in the cell wall of seaweed and form a viscous gel with good adhesion to substrates and cells through chemical interactions [21]. However, the application of cellulose, chitin/chitosan and alginate is highly determined by the specific surface properties, which can be efficiently tuned due to the reactivity and possibility for chemical modification of active surface groups. The surface modification of cellulose and cellulose nanofibers [22], chitin/chitosan [23], and alginate [24], was widely studied by following traditional wet-chemical routes. The functionalization of polysaccharides is particularly interesting in respect to their renewability and offers possibilities for integration in technical applications such as bio- and nanocomposites, films, filter or surgery membranes, adhesives, aerogels, or hydrogels.

The aim of this review is to highlight opportunities for bio-inspired surface functionalization of polysaccharides through the mimicking of mussel-adhesive properties with dopamine. The intense cross-over studies between polysaccharide and protein chemistry were performed in last decade. Starting from the adhesive properties of dopamine, the scope can be broadened towards the creation of a general platform for functionalization of polysaccharides with catechol chemistry. The different functionalities and technical applications covered by mussel-inspired modification of cellulose, chitin and alginate are summarized in **Figure 1**. This review is particularly written in a multidisciplinary approach focussing on chemical mechanisms and engineering aspects of dopamine-modification. After an introduction to the chemistry behind mussel adhesion and dopamine resources, the functionalization of cellulose, chitin and alginate is discussed. Interestingly, the concept of catechol-based surface functionalization can be generalized towards further industrial applications by using synthetic analogues of polyphenolics.



Figure 1. Overview of actual functionalities and technical applications for cellulose, chitin and alginate with mussel-inspired surface functionalization, as covered in this review paper.

2. DOPAMINE RESOURCES AND CHEMISTRY

The ability for mussels to attach onto a variety of substrates is controlled by the existence of so-called byssus filaments, which are protein or “sea silk” fibers connecting the mussel body to a foot plaque. The fibers are primarily produced by young mussels, while some mussel varieties (e.g., *M. Mytilida*, *M. Pinnida*, *M. Arcida*) form the threads over their life-time, and others even construct a full and dense fibrous network. With this structure, the mussel builds strong and reversible underwater adhesion, due to both the mechanical properties of the byssus threads and the chemical composition of the foot plaque with so-called *Mytilus edulis* foot proteins (*Mefp*). The formation of the byssus and secretion of *Mefp* is an essential metabolic activity, as it requires around 12 % of the total body energy [25]. The shell and byssus consume a significant share of the totally generated carbon (8 and 44 %, respectively) and nitrogen (8 and 21 %, respectively) [26]. After the production of *Mefp* inside granules and secretion as a viscous liquid at $\text{pH} < 5$, it solidifies few minutes later in seawater environment ($\text{pH} = 8$).

2.1 Byssus thread

The byssus consists of a bundle with 50 to 100 single elastic collagen fibrils that are grouped within a protein coating, with each fibril having a length of about 2 to 6 cm and diameter of 100 to 200 μm . The byssus contains several domains with its proximal end connected to the stem (near the mussel body), a proximal thread, a distal region connected to the foot plaque, and a primary layer covering the adhering surface (**Figure 2a**). The mechanical stiffness of the byssus thread remarkably varies as it is very weak near the mussel body ($E_{\text{stem}} = 10 \text{ MPa}$), becomes stiffer in the thread ($E_{\text{prox}} = 50 \text{ MPa}$), and has relatively high stiffness near the foot plaque ($E_{\text{dist}} = 500 \text{ MPa}$). With this hierarchical structure, the proximal end can be elongated up to about 300 % and the distal part can be elongated up to about 200 %. The exceptional mechanical properties allow for a reversible attachment, with the interface strength depending on the contact angle between the byssus and the substrate (**Figure 2b**): the detachment of the byssus from the substrate in either orthogonal or parallel direction results in an experimentally measured adhesion force of about 300 N (orthogonal = tensile) or 180 N (parallel = shear) [27]. With a total of about 50 byssus threads per mussel, the adhesive strength for a single foot plaque is about 6 MPa (i.e., 5 to 6 N per thread) [28]. Although this value remains relatively low, the combination of flexibility, tensile strength and deformation of the byssus thread makes it as an interesting structure with reversible adhesive properties under aqueous environment.

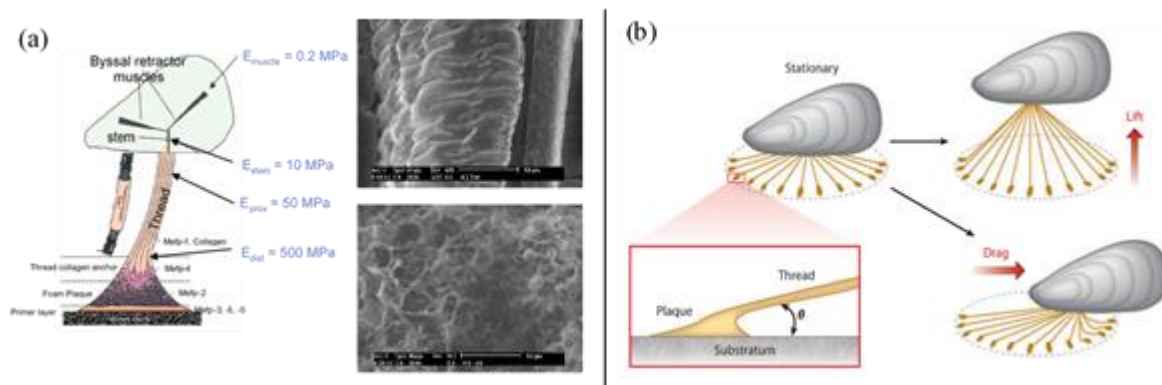


Figure 2. Byssus thread regulating the versatile adhesion of mussels, (a) mechanical construction for the adhesive connection between mussel body and substrate with detail of the collagen fiber in the byssus thread (top image) and detail of the foot plaque providing adhesive properties (bottom image [29] ©2006 reprinted with permission from John Wiley and sons), (b) mechanism for retraction of the adhesive connection by orthogonal or horizontal detachment, taking into account contact angle in the final adhesive force [28] ©2011 reprinted with permission from Annual Reviews.

2.2 Mussel foot plaque as natural resource of dopamine

The adhesive properties of the mussel foot plaque situated at the end of the byssus are governed by an adhesive foam-like substance of different *Mefp*'s. The *Mefp*'s have a decapeptide repeating unit with variable content of the 3,4-dihydroxyphenylalanine (dopa) amino acid, which exists as an enzymatic modification or post-translational hydroxylation of tyrosine as an amino acid precursor. In particular for the blue mussel (*Mytilus edulis*) and Californian mussel (*Mytilus californicus*), the dopa content is high and provides stronger adhesion and deformability than other mussel types. Amongst a range of over 30 different compositions of *Mefp*, the *Mefp-1* to *Mefp-6* are most important and well organized at specific locations in the byssus and foot plaque (**Figure 3a**). In particular, the *Mefp-3* and *Mefp-5* are localized at the outer surface and participate in the adhesion process, in parallel with their composition having high dopa-content (**Figure 3b**). In contrast, the *Mefp-6* and other *Mefp* are located inside the foot plaque and contain lower dopa-content (**Figure 3c**). The compositions of different *Mefp*'s were clarified (**Table 1**), and they are involved in specific functional roles depending on their location [29].

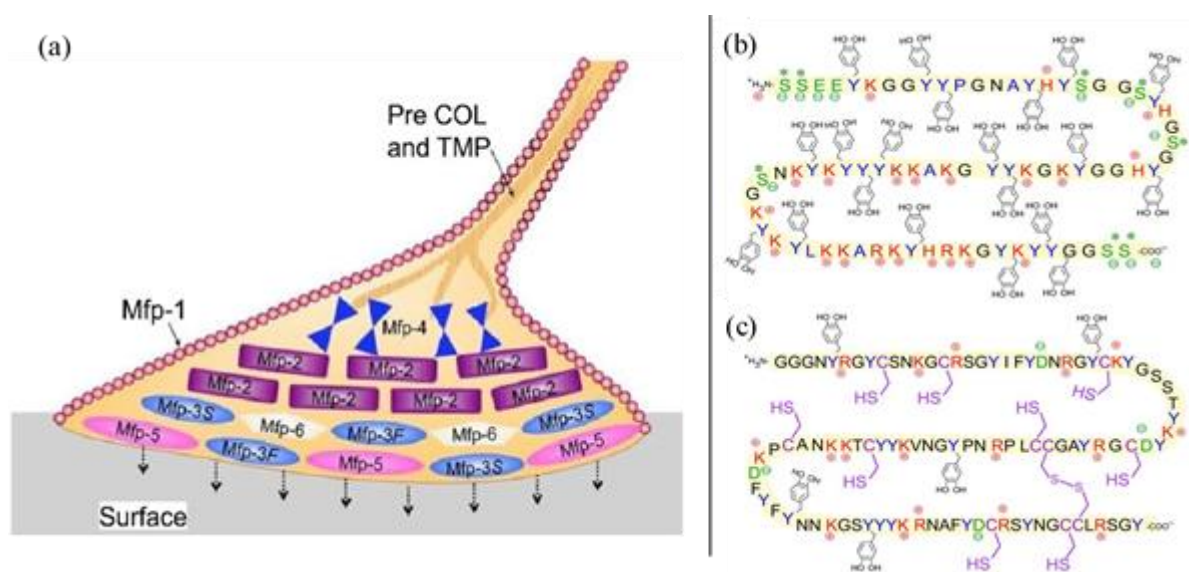


Figure 3. Schematic presentation of the mussel foot plaque with organization of different *Mefp*'s, (a) distribution of *Mefp* in the foot plaque, (b) sequence of *Mefp-5* from *Mytilus edulis* with dopa (Y-methyl catechol), Lys (K), Ser (S) and Gly (G), (c) sequence of *Mefp-6* from *M. californianus* with Cys (C), Arg (R) and Lys (K), Gly (G) and Tyr (Y). Color key: Tyr/Dopa (blue), cationic side chains (red), anionic side chains including phosphoSer (green) and thiols (purple). Sequences from Lee et al., 2011 [28] ©2011 reprinted with permission from Annual Reviews.

Table 1. Mussel foot proteins (*Mefp*) with characteristic composition and location in the foot plaque.

	Mass	Location	Dopa concentration	other prevalent amino acids
<i>Mefp-1</i>	110 kDa	Cuticle	10-15 mol-%	Hyp
<i>Mefp-2</i>	45	Foot plaque core	5 mol-%	Cys
<i>Mefp-3</i>	5 – 7	Foot plaque interface	20 mol-%	HOArg, Asp (15 mol-%), Gly (27 mol-%), Lys, Trp
<i>Mefp-4</i>	90	Foot plaque core	2 mol-%	His
<i>Mefp-5</i>	9 - 11	Foot plaque interface	28 – 30 mol-%	pSer (5 mol-%), Lys (19 mol-%), Gly (20 mol-%)
<i>Mefp-6</i>	12	Foot plaque interface	3 mol-%	Asp (13 mol-%), Gly (14 mol-%), Cys (11 mol-%), Lys (10 mol-%)

Hyp = hydroxyproline, Cys = cysteine; HOArg = hydroxyarginine, Asp = asparagine, Gly = glycine, His = Histidine; pSer = phosphoserine, Lys = lysine, Trp = tryptophan.

The features and biochemical compositions of *Mefp*'s were frequently reviewed [30], and are shortly summarized in this paragraph. The *Mefp-1* is located in the byssus cuticle forming an outer skin of about 2 to 5 μm with multiple layers that are, however, not covalently linked with each other. Therefore, it does not contribute to adhesion or crosslinking of the proteins in the byssus or foot plaque, but it surrounds the core of collagen fibers and protects against microbial attack. The *Mefp-2* is the most frequent protein providing structural integrity to the interior part of the foot plaque. It contains polypeptides that stimulate cell growth (epidermal growth domains) and are stabilized by disulphide crosslinking through oxidation with cysteine. The *Mefp-4* serves as a connecting link between the foot plaque and the distal end of the byssus. It mediates interactions with the *Mefp-2* and collagenous proteins in the byssus by metal ion (Cu^{2+}) coupling in presence of histidine. The *Mefp-6* has similar content of catechol residues than the adhesive *Mefp-3* and *Mefp-5*, but the tyrosine moieties are not effectively converted into dopa. The high content of charged residues and thiol-groups from cysteine in *Mefp-6* provides the ability to control the crosslinking of dopa by disulphide bonding, and it serves as a covalent bonding agent between other *Mefp*. Above all, the most crucial role of thiols in *Mefp-6* exists in creating a redox environment near the foot plaque (i.e., anti-oxidant), which prevents the spontaneous oxidation of dopa into quinone at pH conditions of seawater and maintains the adhesive properties of dopa. In conclusion, the thiol groups allow for a reduction of dopa-quinone into dopa and are responsible for balancing the adhesive and cohesive processes in the foot plaque.

The *Mefp-3* and *Mefp-5* form a primer layer for adhesion at the interface between the foot plaque and substrate. They are particularly characterized by high amount of dopa (20 to 30 mol-%), relatively small molecular weight, and strong hydrophilicity. However, there is a broad variation in composition of *Mefp-3* as the tyrosine residues are partially converted into dopa through a natural post-translational modification,. The *Mefp-5* has higher dopa-content (**Figure 3b**) and is additionally characterized by a significant concentration of cationic charges near lysine, while anionic charges may be introduced through phosphorylation of serine. As such, the *Mefp-5* has a higher polarity and net charge density contributing to better surface adhesion according to various mechanisms: (i) the reactive functionalities may assist chemisorption on polar surfaces, while adsorption may be caused by electrostatic interactions on non-polar surfaces, and (ii) the co-adsorption and aggregation of charged proteins may happen in presence of polyanions [31]. In particular, the position of lysine synergistically controls the catechol interactions by enhancing the surface adhesion and diminishing the Fe^{3+} -mediated cohesion of dopa [32]. It has been proposed that lysine contributes to expel hydrated cations from the solid surface, thereby creating space for the catechol moieties to approach the surface [33]. The self-oxidation of dopa into quinone may be protected in presence of other *Mefp*, although the pH conditions of seawater are favourable for oxidation. Therefore, the natural adhesive mechanisms are controlled by the interplay between various proteins: an experiment with time-dependent in-situ tracking of *Mefp* revealed fast secretion of *Mefp-3* and *Mefp-5*, followed by *Mefp-2* and *Mefp-4* forming the foamy interior [34]. According to other studies, however, the presence of dopa is not a sufficient condition to generate adhesion in contact with an adsorbed protein layer. In particular, other important parameters should be taken into account such as the molecular dynamics of the system, availability of dopa-groups at the surface, conformation of the random-coil protein network and chain segment flexibility [35]. The adhesion mechanisms of *Mefp* in different molecular conformations revealed that the adhesive groups occur at the periphery of the folded molecules and thus become more exposed to the surface [36].

The adhesive and cohesive properties of *Mefp* are driven by complex interactions near the dopa moieties, including hydrogen bonding, metal-ligand complexation (chelation), Michael-type addition, Schiff base reaction and phenol coupling or quinhydrone charge-transfer complexation (**Figure 4a**). In particular, the self-oxidation of dopa into quinone plays a key role and determines the reactivity of dopa. The spontaneous oxidation of the catechol follows a radical reaction scheme with formation of intermediate *o*-semiquinone radicals that are transient and decay rapidly through disproportionation into *o*-quinone and catechol. Although this is a reversible reaction with a low energy barrier, it is thermodynamically unfavourable under environmental conditions. The adhesion is thus balanced by the presence of catechol and quinone, as follows:

- In catechol form, the adhesion is mediated by covalent bonding, hydrogen bonding, or chelation. The metal chelation of dopa occurs in presence of dissolved metal ions (crosslinking), or in combination with metal ions at the substrate (adhesion). The chelation happens with bi-valent (e.g.

Ca^{2+}) or tri-valent (e.g., Fe^{3+}) ions forming coordination bonds with optimized crosslinking and highest strength at a molar ratio $\text{Fe}^{3+}:\text{dopa} = 1:3$ [37]. As such, an octahedral complex forms with three catechol ligands that can be recognized as a red-colored substance. The increase in iron concentration causes a break-up of the crosslinked structure from a tri-complex into bi- and mono-complexes with lower strength and apparent color change into blue or green (**Figure 4b**). The associated color changes occur through an overlap of electrons in free π orbitals of the dopa and free d orbitals of the iron. The crosslinking and adhesion mechanisms by metal complexation depend on the pH, where acid conditions induce the mono-complex formation with low strength and base conditions favour the bi-complex ($5.6 < \text{pH} < 9$) or tri-complex ($\text{pH} > 9$). The pH changes offer a tool for reversible binding in mussel-inspired adhesion systems [38]. Alternatively, less rigid binding of catechol occurs by hydrogen bonding between the hydroxyl groups of the catechol and functional groups at the substrate. The other adhesive interactions also establish through a parallel stacking of the aromatic ring when it is oriented parallel to the surface [39].

- In oxidized quinone form, the Michael-type reaction occurs in presence of nucleophiles and results in the formation of adducts with α,β -unsaturated ketones. Otherwise, the Schiff-base reaction involves the nucleophilic attack of a ketyl group by an amine residue along the protein chain. The mutual interaction or recombination of free radicals between quinone and dopa produces two aryloxy free radicals or semi-quinones that may couple to form a di-dopa biaryl covalent bond. However, the strong tendency for spontaneous oxidation of dopa results in reduced adhesion [40]. Therefore, it remains a most significant challenge for good adhesion to control the redox reaction in a temporally and spatially defined manner [41].

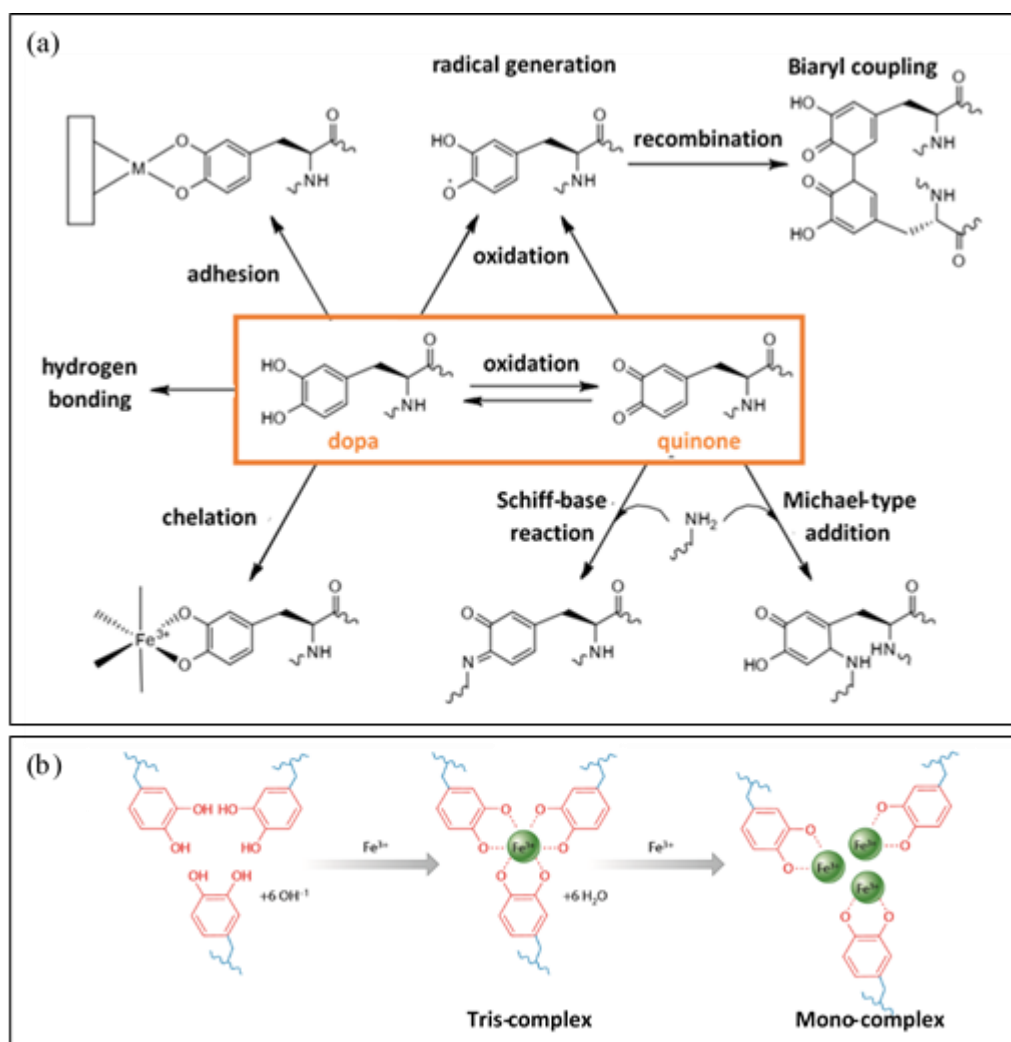


Figure 4. Schematic presentation of chemically controlled adhesive reactions of catechol in biological systems, (a) possible reactions involving adhesive and cohesive bonding at the side of dopa or oxidized side of quinone, (b) mechanisms for crosslinking of dopa catechol by metal chelation and formation of tris-, bis- and mono-complexes depending on the Fe³⁺ concentration. [28] ©2011 reprinted with permission from Annual Reviews.

2.3 Synthetic routes of dopamine

The synthetic production of dopa may follow a top-down approach (e.g., extraction or recombination from its biological host), or a bottom-up approach (e.g., direct chemical synthesis of engineered peptide sequences or macromolecular structures). This paragraph is intended as a brief overview, as the background of dopa biotechnology was covered in excellent reviews [42,43]. While comparing the quality of *Mefp*'s after chemical extraction or recombinant production, the ones extracted from mussels show better adhesive properties, but recombination offers a cheaper alternative with possibility to include additional engineering functions [44]. The chemical extraction from mussels generally results in very low yields as the amount of dopa in the byssus and foot plaque is limited: e.g., the extraction of

Mefp-1 in its full length requires about 10,000 mussels to yield 1 gram of protein [45]. Moreover, the extraction does not provide pure or individual proteins and often requires additional post-processing [46]. The *Mefp-3*, *Mefp-4*, *Mefp-5* and *Mefp-6* were successfully extracted for biochemical analysis on lab-scale, but up-scaling of the production was economically not profitable [47]. In addition, the conversion from tyrosine to dopa is hard to control with a very low yield of only 7 %. A better method for the conversion of tyrosine into dopa was followed by hydroxylation [48], incorporating borate into the reaction mixture together with tyrosinase at relatively high concentrations to avoid the formation of trihydroxy-phenylalanine side products. The hydroxylation is mediated by tyrosinase enzymes in order to retain adhesive properties in a more controlled way [49]. As such, the conversion of tyrosine to dopa can be better controlled by a specific incorporation strategy and an auxotrophic cell line that better recognizes dopa instead of tyrosine during expression [50]. In particular, the DNA code of *Mefp-5* could be isolated and was used for the production of recombinant *Mefp-5*, which was expressed in a soluble form in *Escherichia coli* and was highly purified by chromatography [51]. Alternatively, the recombinant hybrid *Mefp*'s could be synthesized as a fusion protein from different decapeptide repeat units with relatively high yield and purity, using an acetic acid extraction and post-purification in aqueous environment [52]. In general, the recombinant production utilized various heterologous hosts, including bacteria, yeast, insect cells, and mussel primary cells, in combination with a successful post-translational modification of the tyrosine residues into dopa [53].

A common strategy for synthesis of dopa sequences follows the enzyme-induced polymerization of peptides using tyrosinase. As an advantage, it offers facile access to the *Mefp* molecular structure without the complexity of naturally derived proteins. The peptides with a dopa derivate can be synthesized following standard solid-phase methods with high flexibility in choosing sequences, as the side chain deprotection and cleavage from a resin can be accomplished in one step [54]. The synthesis of dopa derivatives can be easily realized by using chemical protection groups, such as a phthaloyl group for the amino group, an acetonide protection of the catechol group, and using the carboxyl group as a methyl ester. After removal of the protecting groups, the intermediates can be converted into Fmoc-dopa(acetonide)-OH and they can be successfully incorporated into short dopa-containing peptides [55]. The dopa-peptides could be attached to anchoring domains of poly-N-substituted glycine oligomers peptoides and effectively served as anchoring points for immobilizing the polymer onto TiO₂ surfaces [56]. Alternatively, the tyrosine sites in peptides were converted by an in-situ oxidation and reduction of the o-quinones, offering high chemo- and region-selectivity of the oxidation reaction [57]. As such, specific peptide sequences could be artificially synthesized as *Mefp* analogues using cysteinyl-dopa linking of the *Mefp-1* decapeptide [58]. However, the peptide length is critical for the efficient adhesive and cohesive interactions of dopa and it is unfavourable in short peptide sequences.

Indeed, the bio-mimetic peptide sequences need to represent the possibilities for coordination bonding of dopa with metal ions, intermolecular interactions due to electrostatic forces, lysine charges, hydrogen bonding and hydrophobic interactions between the aromatics [59]. Therefore, the controlled presentation and access of ligand structures for efficient adhesion needs a model system to define optimized peptide functionality, morphology, distribution and conformation. The grafting of surfaces with peptide ligands or peptide-polymer hybrids meets some of these criteria, but it does not allow for precise control over the synthesis and presentation of dopa. The better defined architectures can be obtained by directed self-assembly of ligand units in the form of so-called “peptide-hybrid materials” [60]. The realization of supramolecular assemblies requires a careful design and choice of distinct sites that regulate the adhesive properties and direct the assembly. For example, the addition of an alkyl chain to the N-terminus of the functional peptide (lipidation) results in a molecular conjugate that is referred to as a peptide amphiphile with hydrophobic and hydrophilic sites [61]. By combining the dopa-peptide sequence with a polymer tail of diacetylene, the linear structures of hybrid polymer-peptide molecules allow for the self-assembly by organization of the hydrophobic tails into 100 nm vesicular structures with the dopa functional groups oriented at the outer surface of the vesicles [62]. The following light-induced polymerization of unsaturated diacetylene bonds allows for stabilization of the vesicles with additional functionalities such as colorimetric and fluorescent response upon temperature, pH, and mechanical stress [63, 64].

In practice, direct chemical synthesis is mostly applied to incorporate dopa groups into polymers. The linear and/or branched copolymers were designed through direct functionalization of the catechol, polymerization of catechol-modified monomers, or use of catechol-functionalized initiators [65]. Some adhesive acrylates (e.g., poly(dopamine-methacryl-amide-co-methoxyethyl acrylate)) were synthesized by free-radical polymerization of the monomers [66], with the disadvantage that the final copolymers are insoluble in water due to a high degree of crosslinking under oxidizing conditions [67]. Therefore, alternative routes were developed with better controllable reactivity under different polymerization conditions of temperature, pH, concentration or UV light. For example, the dopa was incorporated in methacrylate block copolymers by photopolymerization reactions [68-70], in polyethelene glycol copolymers by standard carbodiimide coupling chemistry [71], or in poly(ethylene oxide) copolymers through activation of the hydroxyl end groups by disuccinimidyl carbonate [72-73]. As an advantage, the crosslinking of dopa during heating was avoided while the copolymers form an adhesive gel [73]. In general, a universal affinity fusion tag (e.g. poly-(DOPA)₄-tags) was developed for immobilizing proteins on biomaterials [74]. The modification of polysaccharides with dopa by using *grafting-to* and *grafting-from* with carbodiimide coupling is further illustrated in next paragraphs.

3. POLYDOPAMINE MODIFICATION AND FUNCTIONALIZATION OF CELLULOSE

After extraction of cellulose fibers from various lignocellulosic sources through pulping, subsequent processing steps under mechanical and/or chemical conditions allow to further disassemble the hierarchical fiber structure into its elementary fibrils with nanoscale dimensions. The various forms of crystalline cellulose nanocrystals (CNC), or cellulose nanofibrils (CNF) provide ample opportunities for surface modification and formation of functional materials. A review specifically focussing on dopa-functionalization of lignocellulosic fibers was presented before [75]. In this section, some details on surface modification and technical applications for dopa-modified cellulose are covered.

The abundance and accessibility of hydroxyl groups at the cellulose surface provides good reactivity for covalent binding with polydopamine (PDA) or its intermediate quinone form, according to a Schiff-base or Michael-type addition reaction (see Figure 4). A PDA layer may form through oxidative self-polymerization of dopamine monomers in hydrochloride aqueous conditions, resulting in nanoparticle-like deposits on cellulose fibers. Although the self-polymerization mechanism is not yet fully understood, it includes formation of quinone, internal cyclization into leucodopamine, and subsequent oxidation and rearrangement leading to the formation of dopamine-chrome and indole intermediates (**Figure 5**). The PDA then forms as a copolymerization product with covalent bonds between the latter dimer or trimer oligomers. The PDA layer can be used for the surface modification or as an intermediate activation layer on cellulose fibers.

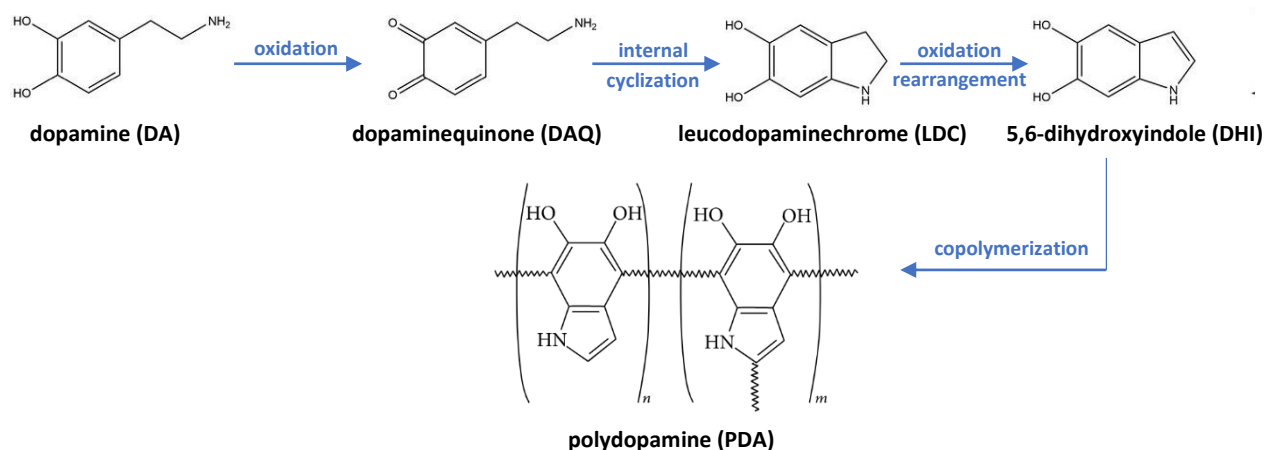


Figure 5. Scheme for oxidative self-polymerization of dopamine into PDA.

3.1 Macroscale cellulose fibers

After coating native cellulose fibers with PDA, the modified fibers gain hydrophobic surface properties and better interface compatibility for their main application as a reinforcement in bio-based composites. As an advantage, the deposition of PDA under mild reaction conditions did not cause any chemical degradation of the cellulose fibers. When mixing with a biopolymer matrix such as polylactic acid

(PLA), the dispersion improved for dopa-modified bamboo fibers [76], or wheat straw fibers [77], resulting in enhanced mechanical properties. A good balance of mechanical properties was achieved, as the PDA layer provides nucleation sites to augment the crystallinity of the polymer matrix, while it also functions as a plasticizer to compensate for brittleness of the reinforced composites [78]. In a novel design for cellulose fiber/polymer matrix interfaces, the dopamine was incorporated into self-assembled adhesive nanovesicles that were deposited on cellulose fibers in aqueous suspension. The local presentation of dopa at the fiber surface enhances the interfacial shear strength and provides additional sensitive properties in order to localize local defects and/or shear stresses in the interface [79].

The dopa-modified cellulose was evidently used in textile applications, providing super-hydrophobicity, anti-microbial properties, photocatalytic activity, electrical and thermal conductivity, fire resistance, or bio-adhesion. The PDA layer on cotton textiles served as an intermediate anchor for the binding of inorganic nanoparticles by an *in-situ* reduction reaction. The catechol groups operated as active sites for chelation and reduction during the deposition of silver nanoparticles from silver nitrate solution [80], copper nanoparticles from sulphate solution [81], palladium nanoparticles from potassium-chloride solution [82], titania nanoparticles from ammonium solution [83], silver/tungsten oxide nanoparticles from chloride solution [84], or bismuth/vanadate core-shell nanoparticles [85]. The presence of a PDA layer improved the adhesion and homogeneous distribution of carbon nanotubes at relatively high concentrations that allow to form an interpenetrating conductive network on cotton [86]. Evidently, the cellulose fibers with PDA can be applied in paper-based materials, incorporating the magnesium nanoparticles and stearates with superhydrophobic and fire-resistant properties [87], or titania nanoparticles with photocatalytic properties [88]. In particular, the addition of paper fibers with PDA during papermaking improves the wet strength of paper sheets and increases the retention of the fiber fines in the paper bulk as a replacement for common retention aids [89].

3.2 Nanocellulose

The functionalization of CNC with a PDA layer created chemical affinity towards different components and introduced hydrophobic properties after subsequent reaction with thiol groups and castor oil [90], or good reactivity towards amino groups [91]. The dopa-CNC provides enhanced surface properties for incorporation into nanocomposite materials by solvent casting. The interface compatibility of dopa-CNC was improved with PVA [92], or PLA [93], while it was also used for the grafting of polyethylene glycol that serves as a plasticizer during processing of the polymer matrix. Besides better chemical compatibility, the porous surface morphology of the PDA layer also stimulates the absorption capacity of dopa-CNC when used as a scavenger for metal contaminants in filtration materials [94]. Alternatively to the organic surface modification, the hybrid CNC nanoparticles with metal nanoparticle deposits could be created by *in-situ* reduction reactions in presence of a PDA interlayer. The dopa-CNC was

modified by deposition and better dispersion of simple metal nanoparticles [95, 96], or metal-organic frameworks [97], as the PDA catechol groups can bind with metal ions and form a metal–catecholate coordination complex. It was not only the adhesion between the metal-oxide framework and cellulose fiber that was improved, but also the crystal growth and crystallinity of the framework was influenced by the nucleation efficiency of PDA.

The direct grafting of PDA was preferentially done for TEMPO-oxidized CNF, or carboxymethylated CNF [98]. As a result, the dispersion and self-alignment of the fibrils could be manipulated by tuning the degree of electrostatic repulsive interactions at certain locations on the CNF surface, while additional crosslinking between the fibrils was established by the complexation with metal ions. The dispersions with organized dopa-CNF could finally be transformed in free-standing films with assembled fibrils providing enhanced optical properties and mechanical performance. Alternatively, the dopa-CNF was incorporated as a reinforcement in fully bio-based nanocomposites with soy protein matrix, where the PDA interlayer allowed to increase the dispersion of high CNF concentrations and helped to control the degree of crosslinking in order to create flexible mechanical properties [99]. In general, the dopa-CNF could be used as a template structure for the controlled growth of a biopolymer network in parallel with the full encapsulation of the reinforcing fibrillar network [100]. As a most important application for biomaterials, the dopa-CNF was transformed into hydrogels that are strengthened by the ability for crosslinking by calcium ions [101], or aerogels with enhanced compressive strength and local receptor sites for adsorption of contaminants [102]. The incorporation of metal particles as a catalyst in dopa-CNF networks or aerogels was favoured by reduced leaching and reversible recovery of the loading after adsorption experiments [103]. The aerogels have a porous structure and were obtained by freeze-drying of the original gel structures with dopa-CNF and replacement of the liquid dispersant by air, however, providing dimensional stability through strong interactions between the cellulose fibrils.

4. POLYDOPAMINE MODIFICATION AND FUNCTIONALIZATION OF BACTERIAL CELLULOSE

The bacterial cellulose (BC) is an alternative source of nanocellulose forming a dense and porous network of thin fibrils with width below 100 nm and diameter of 2 to 4 nm. The BC is secreted by *Acetobacter* bacteria as a cellulose grade with extremely high purity, degree of polymerization and crystallinity. The primary use of BC in wound dressings and clinical applications requires protection with anti-microbial properties and/or functionalization to improve biocompatibility. The common route for deposition of Ag nanoparticles involves the introduction of carboxyl groups by TEMPO-oxidation of BC, followed by an ion-exchange reaction and addition of a reducing agent [104].

Alternatively, the in-situ reduction of Ag nanoparticles on BC with a PDA coating can be done similar to previous procedures for nanocellulose (**Figure 6a**). The soaking of BC in alkaline dopamine solution

was appropriate for the reduction of silver ions from silver nitrate solution, which was even applied in combination with prior deposition of magnetite nanoparticles to combine antimicrobial properties with magnetic response [105]. After deposition of a PDA layer on BC nanocomposite fibers with magnetite nanoparticles, the coating layer became thicker as the self-polymerization of dopamine was likely catalysed in presence of Fe^{3+} . Instead of silver deposition from common silver nitrate solution, also the in-situ reduction from a Tollen's reagent (i.e., $[\text{Ag}(\text{NH}_3)_2]^+$) was proposed to offer lower cytotoxicity [106]. The PDA layer hugely stimulates the growth of fibroblast cells for better biological compatibility of BC. The cell behaviour was due to a combined effect of general adhesive properties and the better control over time-dependent release of Ag^+ from the dopa-BC/Ag fiber network. The wet-adhesion of anti-bacterial patches with PDA evidently improved the skin adhesion. However, significant differences in cell interaction between dopa-BC and more common poly(lactide-glycolide)-BC scaffold membranes were observed during *in vivo* studies [107], indicating lower cell proliferation and collagen accumulation on PDA coatings. The hydrophilic nature of BC and passivation of the PDA layer by proteins could create a layer with a denser microstructure, which did not happen on the more hydrophobic surfaces. The supplementary incorporation of reduced graphene oxide together with silver on dopa-BC composite films further improved the flexibility and toughness of the antimicrobial patches along with thermal or electrical properties (**Figure 6b**) [108]. The free hydroxyl groups in the catechol successfully contributed in the simultaneous reduction of silver ions and graphene oxide, which formed a well-dispersed intercalated structure. The dopa-BC nanocomposites for use as scaffolds presented high ability for mechanical energy dissipation, thermal stability and hydrophilicity in presence of graphene.

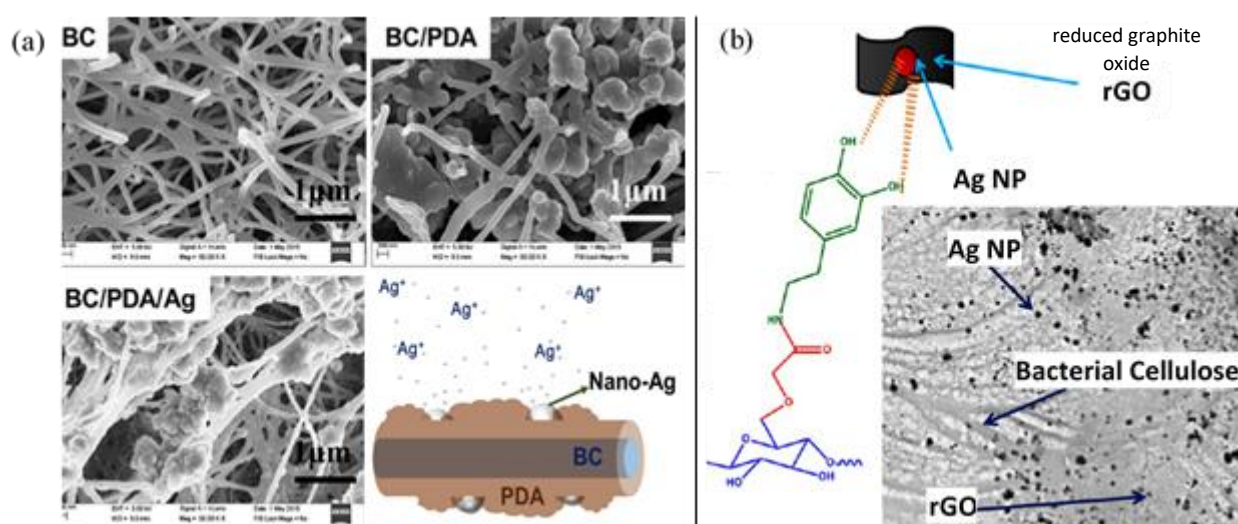


Figure 6. Bacterial cellulose (BC) as functionalized anti-microbial wound dressings with (a) Ag nanoparticle deposits on dopa-BC with controlled release of silver ions [106] ©2019 with permission from Elsevier, (b) combination of dopa-BC with Ag nanoparticles and intercalated graphene oxide sheets [108] ©2019 with permission from American Chemical Society.

The technical applications of dopa-BC as filter membranes are situated in the field of industrial wastewater treatment and are based on the adsorption capacity for specific contaminants such as heavy metals or organic dyes (e.g., methylene blue, rhodamine, or methyl orange). Therefore, the PDA nanoparticles were incorporated as receptors during the in-situ bacterial growth of BC filter membranes [109]. The PDA nanoparticles were first formed in a mixed aqueous solution of hydrochloride and water/ethanol-ammonium [110], and subsequently dispersed in the solution of the bacterial culture and growth media for direct incorporation in the BC fiber network (**Figure 7**). As monodisperse sizes of around 800 nm are required for the efficient trapping of PDA nanoparticles, the particle size could be closely controlled by the ammonia to dopamine ratio. Due to the chelating properties of PDA, the adsorption of metal ions such as Pb(II) and Cd(II) increased, while the π - π interactions between aromatic groups enhanced removal of organic pollutants even after several regeneration and washing steps. The potential of hybrid dopa-BC composite filters for environmental applications (e.g., removal of pesticides, capture of pollutants, decomposition of toxicants, selective gas adsorption and water purification), was generalized by using it as a template for the growth of metal-organic frameworks [111]: the PDA layer generated in-situ crystallization of zeolitic imidazolate nanoparticles, while it also protected against competitive complex interactions between cellulose and zinc ions. The demonstrations for removal of iodine revealed high efficiency of the PDA layer in photothermal regeneration by stimulating the release of captured iodine.

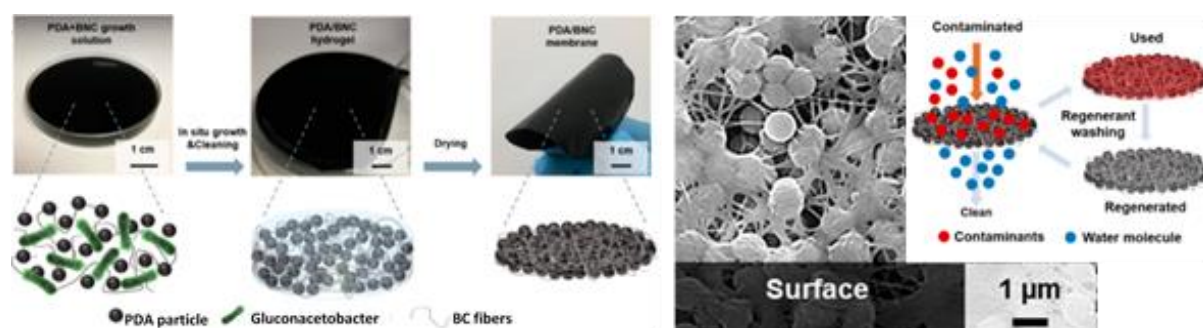


Figure 7. Incorporation of PDA particles in BC fiber network for efficiency as filter membranes for selective removal of contaminants and regeneration [109] ©2019 with permission from American Chemical Society.

The use of dopa-BC in composites for energy production, capture or storage relies on the conductivity or photonic properties of the fibrillar network. As an alternative for polyaniline and polypyrrole conductive polymers, the flexible electrodes of dopa-BC were made by progressive penetration of dopamine in the fiber network and self-polymerization into a granular PDA layer on the fibers, while preventing full agglomeration into a continuous film. Therefore, the polymerization conditions were strictly controlled with low speed under neutral pH (instead of alkaline) and low dopamine

concentration. As such, the BC serves as a three-dimensional template to make a conductive network by exploiting the electronic and ionic conductivity of PDA that operates as an electron-acceptor component and has good ion affinity [112]. There are not yet fixed theories explaining the electronic conductivity of PDA, but the layered structure of π -bond stacking and conjugated chains likely induce similar electronic interactions as in graphite layers. Related to its molecular structure, the other properties of PDA include the absorption of photon-energy and conversion into heat. The presence of PDA particles of around 1 μm in a BC network provides a high degree of light extinction due to internal scattering by the fibers in combination with the light absorption of densely loaded PDA particles [113]. In parallel, the low thermal conductivity of BC and insulating properties of PDA minimize heat loss and localize the generated heat at the surface. Owing to the high water absorption capacity of cellulose, the dopa-BC was used as an efficient solar steam generator under sunlight irradiation. The dopa-BC are ideal candidates for generation of carbon nanofibers by carbonization or pyrolysis, with excellent performance as supercapacitors due to high surface wettability and conductivity [114]. However, dopa-BC would be a much better candidate for fabrication of nitrogen-doped carbon fibers (which are now formed under ammonium activation [115], or nanoporous carbon [116], as the N-doped carbonaceous materials raised increasing interest for application in batteries, catalysis, CO_2 adsorption and electronics with better performance than pure carbon materials.

5. POLYDOPAMINE MODIFICATION AND FUNCTIONALIZATION OF CHITOSAN

Chitosan is a linear polysaccharide of covalent $\beta(1\rightarrow4)$ -linked units of acetylated parts (N-acetyl-D-glucosamine) and deacetylated parts (D-glucosamine), which is prepared by the deacetylation of naturally occurring chitin primarily composed of N-acetylglucosamine. The main polymer backbone of chitin is comparable to cellulose, while one hydroxyl side group is substituted by an acetyl amine group. The solubility and processing of chitin is limited and requires a certain degree of conversion or deacetylation in presence of sodium hydroxide, which renders a soluble product in acidic environment. The chitin naturally occurs as a main constituent in exoskeleton of crustaceans and insects, or in the cell walls of fungi.

In certain marine invertebrates (e.g., hydroid perisarc), a spectacular example of a natural hierarchical composite structure of dopamine and chitin is found: a sheath of chitin fibrils is embedded in a matrix of proteins and oxidized dopamine, and it forms a load-bearing tissue material with high hardness, stiffness and toughness under wet conditions [117, 118]. The other invertebrates (e.g., jumbo squids) are also composed of chitin, proteins and dopamine pigments that occur in an ordered framework [119]. The formation of a network between iron complexes with the dopamine and crosslinking of the proteins by the catechol groups play a possible role in the mechanical stiffness and toughness. In particular, the density of the protein matrix increases with dopamine crosslinking, which provides high stiffness under

wet conditions for fully non-mineralized biological structures. As such, the creation of structures with a functional gradient in crosslinking density may contribute to a high stiffness. In a first step for synthetically functionalizing chitosan with dopamine, however, it has been recently noticed that the synthesis conditions hugely affect the state of oxidation of the catechol (**Figure 8**). The interaction between the catechol and amine groups in the chitosan backbone particularly depends on the formation of quinone and/or side-products such as catechol-amine adducts [120]: the occurrence of different conformations are pH-dependent and may also influence the final adhesive properties. Whereas the catechol exists in its reduced form at $\text{pH} < 5.5$, it oxidizes into a more reactive quinone at higher pH and further polymerizes through formation of covalent crosslinks between dicatechol dimers, primary amines and thiols. The grafting of the reactive *o*-quinone onto the primary amine of the chitosan is a complex combination of Michael addition / Schiff base reactions, and not yet fully characterized [121].

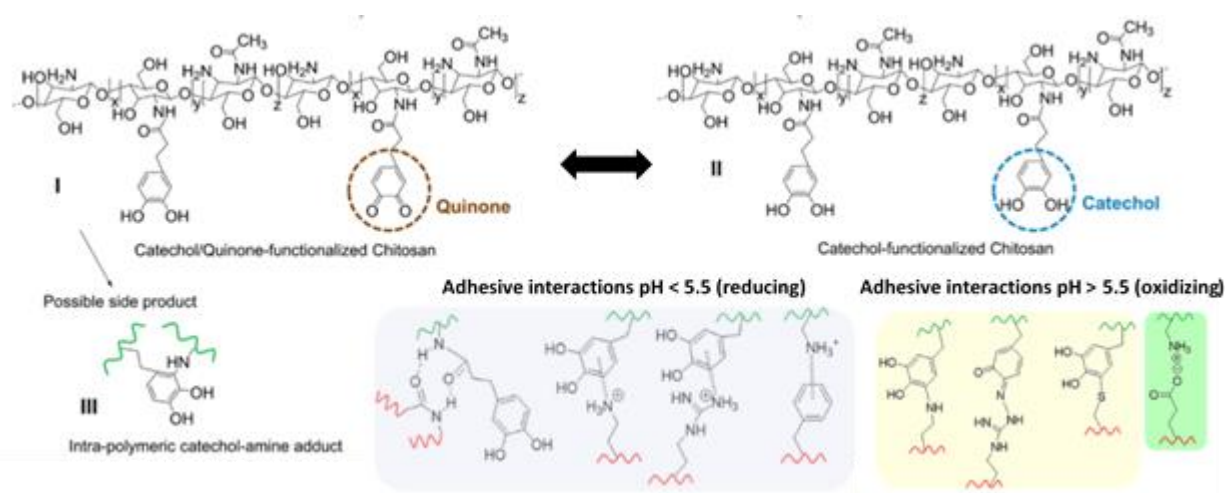


Figure 8. Functionalization of chitosan resulting in different products depending on pH conditions (reductive catechol/oxidative quinone) and impact on the formation of adhesive interactions [122]: electrostatic interactions at $\text{pH} < 5.5$ (in blue), covalent bonding at $\text{pH} > 5.5$ (in yellow), additional electrostatic interactions between carboxylates and amines at $\text{pH} > 5.5$ (in green) ©2019 with permission from Americal Chemical Society.

5.1 Biocomposites and nanocomposites

The examples of biomimetic design with chitosan/dopamine composites provide inspiration for the fabrication of synthetic lightweight and biocompatible composites with tunable mechanical properties [123]. As such, one drawback of chitosan can be resolved, i.e. the poor mechanical properties under wet conditions due to high moisture uptake and swelling. The mixing of dopamine in chitosan biocomposites served as a crosslinking agent in presence of sodium periodate as an oxidant [124]. The oxidation of dopa resulted in the formation of a melanin derivate that was distributed throughout the

chitosan film and covalently coupled to the amine groups of chitosan. In parallel to a mechanical reinforcement with high stiffness and toughness under dry and wet conditions, the hydrophobic properties improved while the solubility in acetic acid and water absorption decreased. In a further design, the degree of crosslinking between the chitin nanofibers and protein matrix could be spatially controlled and resulted in composites with a gradient in tunable mechanical properties ranging from soft to hard. The degree of crosslinking was controlled through local variations in the concentration of chitosan, dopamine and oxidant, resulting in the formation of catecholamines [127]. During the self-polymerization of dopamine, the simultaneous depolymerization and amorphization of chitosan may contribute to a variation in mechanical properties. The other studies indicated that the conjugation of dopamine with chitosan by grafting through carbodiimide chemistry significantly reduces the rigidity of the chitosan backbone due to the break-up of internal hydrogen bonds, thereby contributing to a much better water-solubility for further processing. The mechanical properties are indeed influenced by the addition of fillers in chitosan nanocomposites, where the dispersion and interface compatibility between nanofillers and chitosan matrix improve with dopamine. The modification of montmorillonite clay with PDA was efficient in promoting the exfoliation of the clay and homogenizing the dispersion in a chitosan/starch film [128]. The better dispersion of modified clay in the chitosan film resulted in better mechanical properties due to the chemical binding between the N-H chitosan functionalities and catechol OH groups, while the total crystallinity of the films remained unaltered. Interestingly, the exfoliation of the dopa-clay particles increased with dopamine concentration and the opening of the layer spacing was favourable for the intercalation of chitosan through an ion exchange mechanism.

The hybrid chitosan composites can be synthesized through coordination bonding with inorganic nanoparticles in order to bring, e.g., magnetic functionality and stimuli-responsiveness. In one approach, the compatibility between iron oxide nanoparticles within chitosan nanocomposites was obtained by dopamine-functionalization of the chitosan matrix [129]. The catechol groups were grafted to the chitosan chain through an amidation reaction in order to reduce the number of hydrophilic amine residues and to provide side groups for subsequent coupling and crosslinking (**Figure 9a**). Therefore, the cured composite films presented favorable mechanical stiffness and hardness under hydrated conditions with high load bearing capacity. The other way round, the chitosan nanocomposites with iron nanoparticles were obtained by functionalization of the nanoparticles. The surface functionalization of iron oxide nanocubes with catechol-chitosan enhanced the dispersion and colloidal stability in aqueous solutions while maintaining a narrow particle-size distribution. The chitosan oligomers with relatively low molecular weight were particularly used for the surface coating of nanoparticles, providing only a thin layer and multivalent binding of dopa-chitosan to iron oxide surfaces. The nanocomposites were used as a biocompatible medium with low cytotoxicity and serve as a drug delivery vehicle for loading and release of the dopamine as active ingredient from the chitosan matrix [130], or as a magnetic heat mediator for local cancer cell treatment [131]. The magnetic dopa-chitosan nanoparticles simultaneously

have higher affinity for adhesive coupling with proteins or enzymes [132]: e.g., the immobilization of transaminase improved the pH activity and thermal stability compared to free enzymes for pharmaceutical or regenerative applications (**Figure 9b**). The dopa-chitosan conjugates thus allow to control the formation and stabilization of nanoparticles dispersed in aqueous media, and act as a mediator for nanoparticle functionalization with, e.g., proteins or peptides.

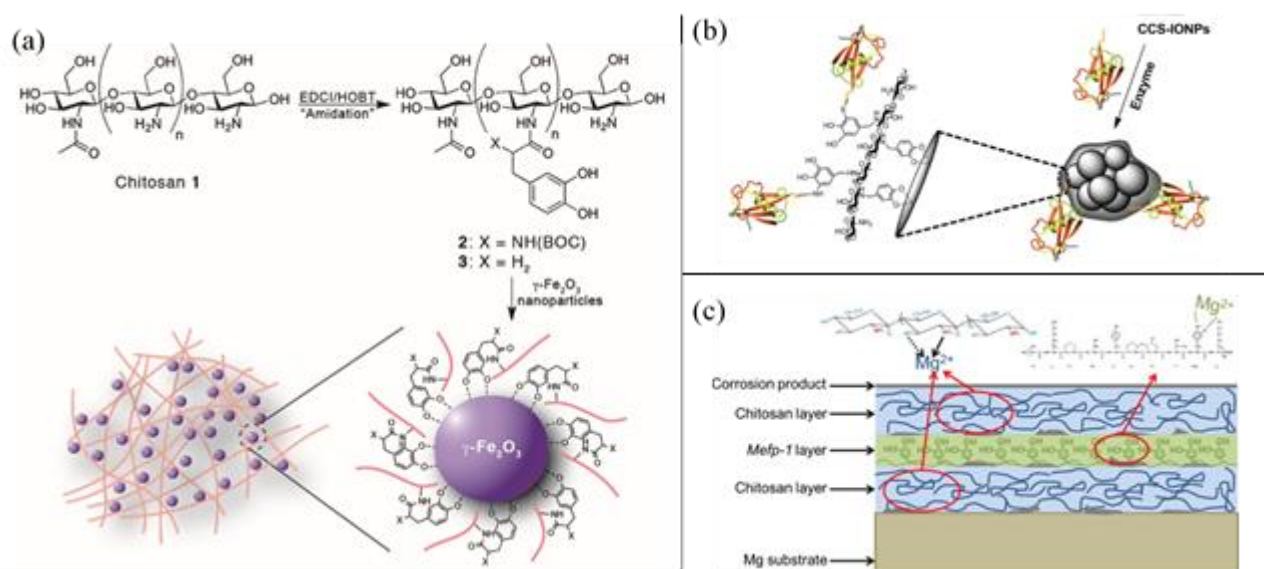


Figure 9. Functionalized dopa-chitosan for bio-based (nano)composites in biomedical applications, (a) encapsulation of magnetic nanoparticles by functionalization of chitosan polymer [129] ©2013 with permission from American Chemical Society, (b) tuning interaction between magnetic metal nanoparticles and enzyme environment [132], (c) corrosion protection of magnesium substrate through alternating dopa/chitosan coating [133] ©2013 with permission from Elsevier.

The formulation of chitosan biomaterials has been favoured in presence of dopamine, facilitating the coupling with biomolecules, encapsulating active ingredients, or improving the biocompatibility and corrosion resistance in contact with body fluids. The electrodeposition of a composite coating with multiple layers of dopa and chitosan onto metal substrates formed a compact anti-corrosion coating due to the synergistic reaction of dopamine and chitosan with chelated magnesium ions (**Figure 9c**) [133]. The growth of calcium phosphate nanoparticles for tissue generation could be better controlled and particle sizes remained limited as the dopa-chitosan layer on calcium phosphate nano-aggregates serves as a particle stabilizer [134]. The chitosan with grafted dopamine was directly added into the growing aqueous alkaline solution of the calcium phosphate with particularly good affinity between the dopamine and divalent calcium ions. The cationic dopa-chitosan could also arrange as a polyelectrolyte complex and thus formed micellar structures with encapsulated DNA molecules through self-assembly via weak

hydrophobic interactions. In presence of amino groups, the chitosan behaves as a cationic polyelectrolyte that assembles with nanoliposomes into particles for protein and drug delivery [135]: the chitosan coating on the liposome particles improved the uptake of levodopa from liposomes due to high biocompatibility and induced less clinical side-reactions. As such, a variety of individual nanoparticle complexes can be synthesized by self-assembly of dopa-chitosan and coordination of various ligands, in order to serve as drug carriers [136]. The surface immobilization of a chitosan layer onto metal nanoparticles is a way to produce functionalized nanoparticles with colorimetric or fluorescent properties for biosensing, where the coupling between the chitosan-coated gold nanoparticles and functional peptides is mediated by dopa-quinone intermediates [137]. In general, the enzymatic conjugation of proteins, peptides, sugars or biomolecules with metal nanoparticles is an important feature for bioassays, where the dopa-linkage provides a flexible link for capture (immobilization) and release (hydrolysis) of the target molecules on chitosan nanoparticles.

5.2 Antibacterial properties in biotechnology and filtration

The intrinsic antimicrobial and hemostatic properties of chitosan are attractive for biomedical applications (e.g., wound dressing, tissue), but the interaction of dopamine with the amine groups of chitosan may likely alter its antimicrobial performance. Indeed, the primary interaction between the anionic bacterial cell membrane and protonated amine groups is the main mechanism of antibacterial activity, whereas the presence of catechol groups may enhance the resistance against bacteria [138]. Therefore, the anti-oxidant properties of dopa-chitosan contribute to a better performance in wound healing applications. The role of dopamine in antimicrobial activity can be partly attributed to (i) better water-solubility of dopa-chitosan and consequently more efficient interaction of the chitosan polymer chains with the bacteria, or (ii) intrinsic antimicrobial properties of some catechols on a molecular level by changing the permeability of the bacterial cell membrane through fatty acid interactions.

The antimicrobial properties of dopa-chitosan are further enhanced by the incorporation of silver nanoparticles. The simple mixing of a dopa-chitosan solution with silver nitrate solution resulted in a core-shell structure of silver nanoparticles with a surface coating [139]. The continuous films of chitosan with silver nanoparticles were developed through layer-by-layer (LbL) deposition from polyelectrolyte solutions, growing films with simultaneous bio-active, antimicrobial, biodegradable and adhesive properties for tissue applications [140]. Depending on the sequences of LbL layers with chitosan, dopa-chitosan, hyaluronic acid and nanoparticles, different interaction patterns were established (**Figure 10**). The interlayers of dopa-chitosan enhanced the internal adhesion through interaction with either the deposited chitosan layer or the silver nanoparticle layer. Also the possibility for crosslinking in a post-processing step provides mechanical reinforcement to the films to act as free-standing materials. Depending on the deposition method, the morphology and wettability of dopa-chitosan films could be adapted [141]: the interdiffusion of different polyelectrolyte layers was lower and the structure was more

homogeneous after spin-coating compared to dip-coating, while the spin-coated films present higher thermal stability, stiffness and lower swelling. Although the adhesive properties somewhat decreased after incorporation of the silver nanoparticles, there was a synergistic effect of silver and catechol on the film stiffness [142]. Alternatively, the silver nanoparticles could be separately coated with catechol-conjugated chitosan in order to enhance antibacterial properties [143]. Interestingly, the silver and chitosan components are active against specific species and are more toxic against gram-negative than gram-positive bacteria. Due to various interactions with the bacterial cell membrane, the specificity can be tuned depending on the design of the composite nanoparticles.

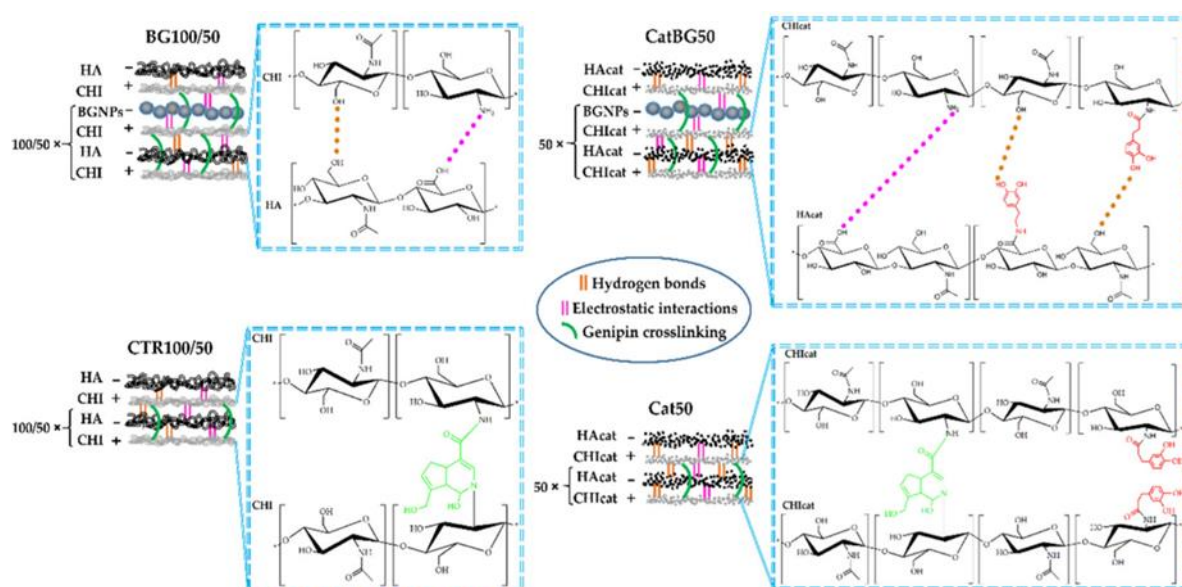


Figure 10. Assembly of free-standing chitosan composite filter membranes with incorporated nanoparticle layers providing enhanced antimicrobial properties by LbL assembly of chitosan / hyaluronic acid / nanoparticle layers [142].

The antibacterial properties are particularly important for applications in (ultra)filtration membranes build from nanoporous filters of chitin nanocrystals (**Figure 11**). After deposition of a PDA layer on the nanocrystals, a relatively high concentration of 57 wt.-% silver nanoparticles could be intercalated within the chitin nanocrystal matrix by in-situ reduction from silver nitrate solution [144]. The membranes were fabricated by a vacuum-filtration of the dopa-chitosan nanocrystals, where the immobilized Ag nanoparticles enabled the creation of a more porous structure with multiple interconnected pores, in contrast to the more compact structure of pure chitosan filtration membranes. As such, the low-resistance channels increased the permeation flux during a continuous flow of the solvent and catalytic functionality was added for removal of organic pollutants or ion recovery.

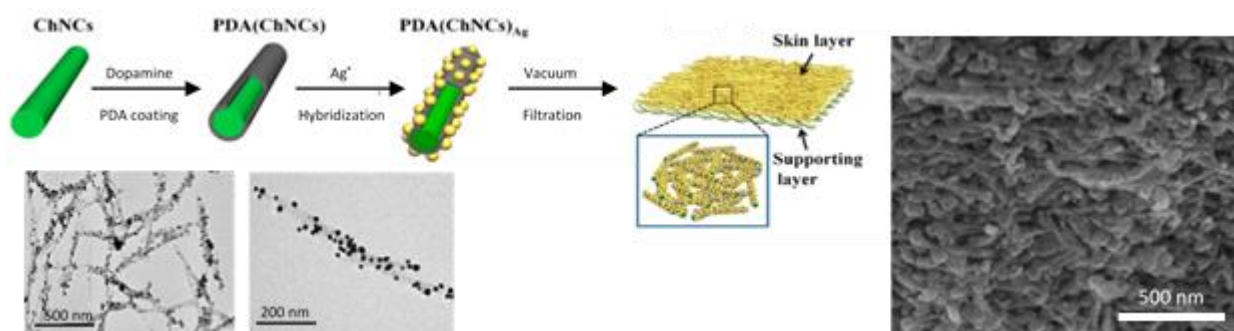


Figure 11. Fabrication of ultra-filtration membranes containing dopa-chitosan nanocrystals and deposition of silver nanoparticles by in-situ reduction reaction, followed by vacuum filtration [144] ©2017 with permission from American Chemical Society.

5.3 Bio-adhesives

The primary application of catechol-conjugated chitosan complexes lies in the field of bio-adhesives for biomedical applications [145], operating under wet conditions in presence of body fluids or hydrophilic components. The availability of both amine and catechol groups allows for a combination of reversible bonding via electrostatic and hydrogen bonds (amines), together with the formation of covalent bonds (catechols). As such, the solidification of dopa-chitosan adhesives can be triggered by crosslinking with catechols, resulting in high cohesive and adhesive strength [146]. In general, the mechanical properties of dopa-chitosan adhesives improve by catechol-amine crosslinking under wet conditions and transfers into a higher strength after drying, which could supplementary be augmented by further oxidative crosslinking [147].

The adhesive surface layers can easily be prepared according to different processing routes such as electrochemical deposition from alternating chitosan and catechol solution [148], or drying and chemical oxidation of a solvent mixture with chitosan, catechol and sodium periodate oxidant [149]. The adhesives with a rather porous structure can be created after freeze-drying of water-soluble dopa-chitosan derivatives (**Figure 12a**), forming a solid three-dimensional network with isotropic diffusion properties and good dimensional stability after crosslinking [150]. The porous adhesive layers are primarily used for bonding to tissue through mechanical interlocking. The development of both cohesive and adhesive strength can be further triggered in combination with a photochemical reaction [151], where the dopamine acts as a photosensitive site under illumination with green light (**Figure 12b**). The photochemical crosslinking then starts from a singlet oxygen created by an initiator (e.g., rose Bengal dye), facilitating the oxidation of dopa through radical reactions. The subsequent crosslinking and covalent bonding between tissue collagen and the amino groups of chitosan occur through (i) Michael addition, (ii) oxidation into a dopa-oligomer network, (iii) Schiff-base reaction, or (iv) direct

crosslinking between tissue and amino groups of the chitosan. As such, efficient photochemical crosslinking excludes the need of chemical crosslinking agents in tissue engineering.

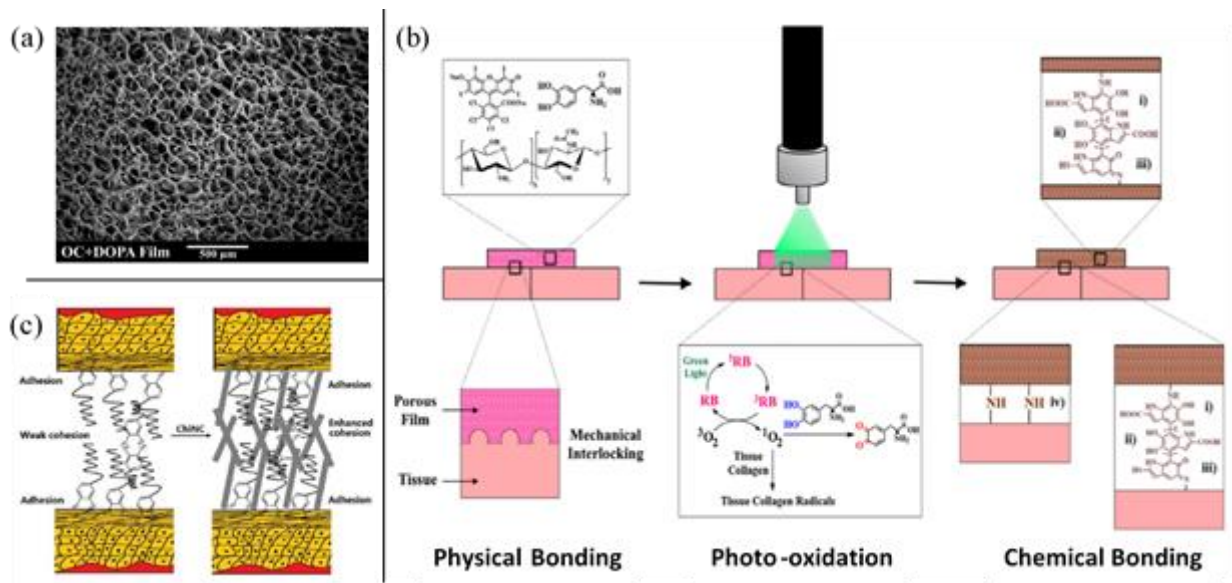


Figure 12. Synergistic role of dopamine and chitosan in enhancing bio-adhesive properties, (a) formation of a porous adhesive dopa-chitosan film with adhesion through mechanical interlocking [150] ©2015 with permission from Elsevier, (b) contribution of photochemical reaction in adhesive tissue bonding shows possible bonding mechanisms for the porous dopa-chitosan films on tissue [151], (c) mechanistic contribution of chitosan nanocrystals in adhesive strength [152] ©2018 with permission from Elsevier.

Besides the occurrence of adhesive films or surface layers, also the nanoparticles with dopa-chitosan adhesive groups may present spectacular increase in adhesiveness compared to pure chitosan particles [153]. The effects of adding chitosan nanocrystals on the adhesive properties of dopamine illustrated that they were finely dispersed in the matrix and stimulated the crosslinking resulting in better strength of the adhesive bond [152]. In general, the consumption of catechol groups to establish internal strength of the adhesive through crosslinking would be in competition with a reduction in adhesive strength. However, an optimum balance could be obtained through the presentation of catechol groups and crosslinking in presence of chitosan nanocrystals (**Figure 12c**). The latter was also an advantage to reduce the swelling of the adhesive layer due to good dispersion and firm chemical embedding of the nanocrystals in the adhesive matrix.

5.4 Hydrogels

Despite the low solubility of chitosan in water, the chitosan hydrogels are highly demanded for biomedical applications (e.g., drug delivery or tissue engineering). The hydrogels consist of a highly crosslinked three-dimensional polymer network as a dispersed solid phase in water. While the chitosan hydrogels are typically prepared via protonation of the amine groups under acidic dissolution, the pH stability is limited and the acid conditions may be toxic to encapsulated ingredients. After derivatization of the chitosan with dopamine through covalent grafting, the water-solubility of high-molecular weight chitosan significantly improves depending on the degree of catechol substitution [154]: the relatively low catechol concentrations (< 7%) could simultaneously retain the intrinsic properties of chitosan, while the small molecular size of the catechol did not block the molecular recognition of chitosan by the cells nor did the catechol provide steric hindrance for cell interactions. As such, the dopa-chitosan hydrogels with high stability were favourably formed under neutral aqueous conditions.

The performance of dopa-chitosan hydrogels in terms of surface adhesion and mechanical properties can be varied according to the crosslinking mechanisms. The adhesive properties of dopa-chitosan hydrogels importantly increased the intrinsic mucoadhesion properties of chitosan polymers, due to confinement of the adhesive catechol groups [155]: as a result, they served as an enhanced carrier for drug delivery. The mechanical properties of dopa-chitosan hydrogels are controlled by either chemical oxidative crosslinking or metal-ion complexation. The chemical oxidation with periodate provided much higher storage modulus, thermal stability and lower swelling than Fe^{3+} triggered crosslinking [156], as expected for covalently bonded dopa-chitosan hydrogels. The control of gelation time and degree of crosslinking is important to maintain good hydrogel functionality. The variation in molar ratio of oxidizing catechol groups is a good parameter to delay the gelation time, but it can also lead to a reduction in final strength. Therefore, a better control over partial oxidative conversion of the catechol under catalytic conditions allows to form quinone intermediates in the solution state, while it only transfers after certain time into the gel state [157]. As such, the gelation is controlled and triggered by catechol-amine crosslinking in order to keep good processing and handling of the hydrogel (e.g. by injection). The resulting hydrogels generally employ the dopamine as a crosslinker, however this would reduce the availability of catechol groups to mediate the mucoadhesive properties. The latter are mainly governed by inter-molecular hydrogen bonding and electrostatic interactions between the chitosan and mucin. Therefore, the non-toxic genipin was added as a compatible natural crosslinker for gelation. The additional crosslinker consumes the amino groups instead of catechol groups, which provided similar mechanical properties compared to pure chitosan hydrogels. The high density of dopa-chitosan hydrogels compared to chitosan hydrogels is favorable for slowing down the degradation process and prolonging eventual drug release. Although the traditional crosslinking of dopa-chitosan hydrogels by oxidation or Fe^{3+} coordination ions provides brown color, reversible coordination bonding with other metal ions such as Al^{III} , Ga^{III} or In^{III} is an alternative to maintain transparency [158]. The brown color

originates partly from (i) transitions in the d-orbitals of the electronic structure in the metal ions, and partly from (ii) the catechol oxidation. Thus, it can be avoided by the selection of metal ions with appropriate structure and/or reducing the degree of oxidation. The presence of semi-quinone species could be controlled by the amount of Fe^{3+} crosslinker relatively to the number of catechol groups grafted onto chitosan or by regulation of pH [159].

The self-healing properties of dopa-chitosan hydrogels can be regulated by the reversibility of metal coordination bonding. However, the various metal ions have different affinity to catechol and may influence the storage modulus of the hydrogel with a significant delay in self-healing [158]. Therefore, other self-healing mechanisms with reinforcing graphene oxide nanofillers were investigated (**Figure 13**), providing simultaneous conductive, self-adhesive and recovery properties for electro-active tissue engineering applications [160]. The graphene oxide was reduced via intercalation during the oxidation of dopamine, while forming a PDA layer that improved the dispersion of the graphene filler and acted as a crosslinker for gelation of the chitosan hydrogel. The reduction of graphene oxide and penetration of PDA in between exfoliated structure also produced some nanofibrils. Therefore, they stimulate the molecular interaction between the chitosan and graphene sheets enhancing mechanical strength, or act as bridges facilitating the self-healing process. The self-healing properties of a dopa-chitosan hydrogel depend on the number of available catechol groups needed for the self-healing process, while a degree of irreversible covalent crosslinking of catechols is required to provide sufficient stiffness. Therefore, a system of double crosslinked hydrogels with metal coordination (reversible) and covalent oxidation (irreversible) was developed [161].

The additional functions such as thermo-responsive properties of chitosan hydrogels were incorporated through coupling of the dopa-chitosan with thiolated block copolymers [162], or a glycerol-phosphate [163]. The permanent binding between catechol groups on the chitosan and hydroxyl groups in the phosphoric acid enhances the incorporation of thermosensitive moieties into the hydrogel without significantly affecting the gelling conditions. The working principle of thermal response relies on the sol-gel phase transition of the hydrogel that should happen under physiological temperatures, e.g. where a gel is formed in contact with the skin. In that respect, the gelation time of dopa-chitosan hydrogels decreased progressively with the higher concentrations of dopamine between 0.5 and 2 %. Simultaneously, the pore structure became more homogeneous and formed a regular array with high specific surface area as the dopamine concentration increased. Based on its redox-active properties, the dopa-chitosan hydrogels were fundamentally studied on a molecular scale with electron-donor, electron-storage and electron-acceptor properties, thus offering redox-capacitor capabilities for information processing in electrochemical processes or electronic circuits [164]. It can therefore be concluded that dopamine modification of chitosan hydrogels does not interfere with the original benefits of chitosan, while it further optimizes the compatibility and functionality for biomedical applications.

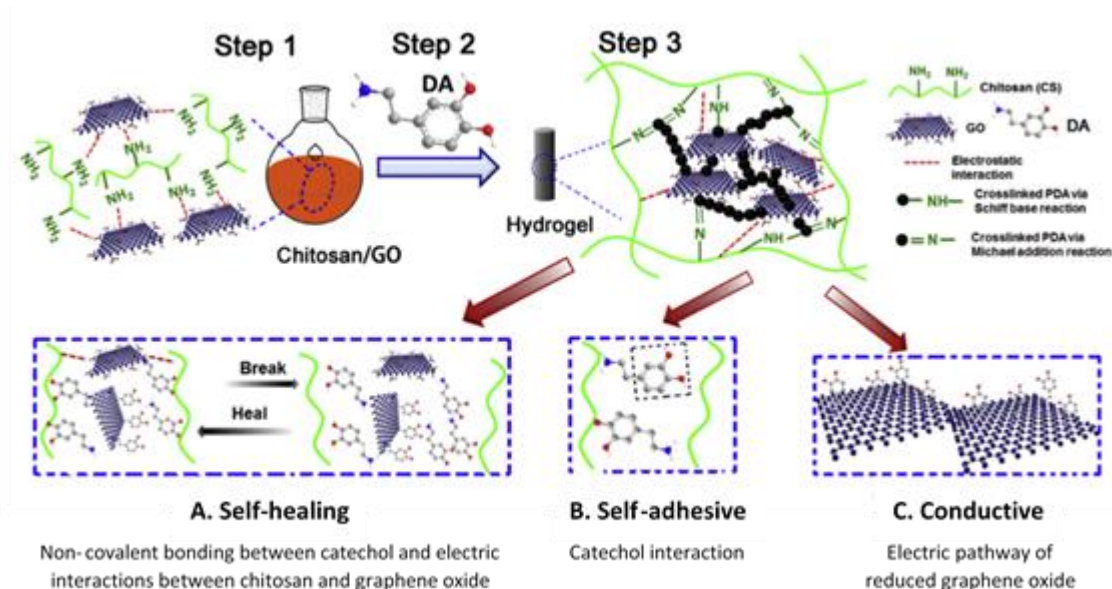


Figure 13. Creation of multi-functional dopa-chitosan hydrogel with incorporation of graphene-oxide sheets providing (A) self-healing, (B) adhesive and (C) conductive properties, formed during step 1 (electric interaction between chitosan and graphene oxide), step 2 (introducing dopamine into chitosan/graphene oxide solution), step 3 (covalent bonding and self-polymerization of dopamine into a composite hydrogel) [160] ©2017 with permission from Elsevier.

6. POLYDOPAMINE MODIFICATION AND FUNCTIONALIZATION OF ALGINATE

The alginate (Alg) is a salt from alginic acid that originates from the cell walls of marine plants such as brown seaweeds as a main source, or bacteria. It consists of a linear unbranched polysaccharide with monomer blocks of (1 → 4)-linked β -D-mannuronic acid (M) and α -L-guluronic acid (G). The polymer composition includes three different sequences of (i) consecutive G-residues, or (ii) consecutive M-residues (homopolymer), or (iii) alternating MG-blocks (copolymer) with different molecular weights and G/M ratios depending on the natural source and species. The use of Alg in biomedical sciences is prompted by its low toxicity, biocompatibility, haemostatic properties and easy gelation in presence of bivalent cations like calcium. Besides the traditional ionic crosslinking, also covalent crosslinking with di-amines or thermal gelation with acryl-amide is possible. As a highly hydrophilic polysaccharide with huge amount of carboxyl groups, the Alg is mostly converted into a porous hydrogel with structural compatibility to biological matrixes for wound healing, microencapsulation, drug delivery, or formation of three-dimensional scaffolds for bone and soft tissue engineering. However, the performance of Alg hydrogels as tissue adhesive remains inferior and it needs to be blended with polymers such as gelatin or chitosan. The role of dopamine was experimentally proven to enhance biological compatibility, mechanical robustness and adhesiveness of alginates under aqueous condition, together with other

properties such as entrapment of functional molecules, self-healing, and selectivity of filtration or surgery membranes.

The modification of Alg with dopamine allows to regulate a good balance of mechanical and adhesive properties in tissue materials due to catechol interactions, improving its applicability and spreading over the contact surface. In particular, the ionic crosslinking of dopa-Alg hydrogels through coordination bonding with iron ions enables the fabrication of underwater glue [165]. In contrast, the conventional adhesive methods utilize the chemical conjugation and covalent binding of the catechol that pose limitations on the chemical synthesis. The good underwater adhesive performance was achieved by subsequently supplying the ingredients towards the submerged interface of different substrates and in-situ pull-off tests. Alternatively, the grafting of dopamine on oxidized alginate may happen through an Schiff-base amination reaction between the amine (dopa-side) and aldehyde (Alg-side), possibly generated in the Alg backbone through partial oxidation [166]. Better adhesion of tissue is then governed by direct interaction of oxidized dopamine in the modified alginate gel and the amine groups in the tissue, while simultaneously increasing the cohesive strength by internal covalent crosslinking (**Figure 14a**). After incorporating poly(lactic acid) nanoparticles in the dopa-Alg hydrogel, they contributed in the formation of a polymer network through reaction with the amine and catechol groups, which may limit the diffusion and leaching of nanoparticles towards the tissue (**Figure 14b**). It was favourably noticed that the catechol groups also serve as a covalent crosslinker for dopa-Alg hydrogels in absence of calcium ions [167]. The concentration of grafted dopamine could be easily controlled by altering the molar ratio of Alg and dopamine up to 40 %, which results in a gradually higher degree of crosslinking and adhesive strength during lap-shear testing. Indeed, the type of failure in bonding pairs evolved from adhesive failure for the original Alg hydrogel into a more cohesive failure for the oxidized hydrogel. Interestingly, the swelling and visco-elastic properties of the dopa-Alg hydrogels with dopamine crosslinking become readily tunable, which is difficult to achieve in traditional Alg hydrogels with ionic bonding. Therefore, the catechol crosslinking provides straightforward control on the microporous structure of dopa-Alg hydrogels, which becomes finer compared to calcium ions (**Figure 14c**).

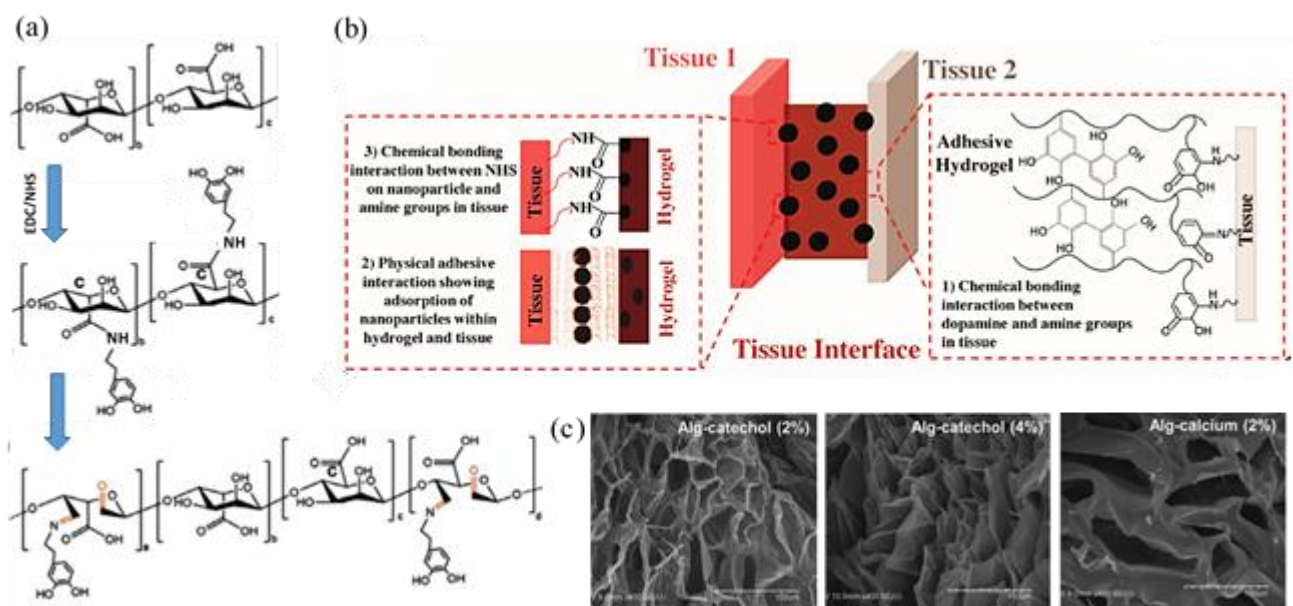


Figure 14. Enhancing mechanical and adhesive properties of dopa-Alg hydrogel with dopamine modification through grafting or Schiff-base amination in combination with partial oxidation, (a) reaction scheme for alginates, (b) interface interactions in adhesive tissue joint with synergistic effect of added organic nanoparticles^[166] ©2018 with permission from John Wiley and Sons (c) porosity control of the Alg-hydrogel under dopamine crosslinking [167] ©2013 with permission from American Chemical Society.

The additional features of dopa-Alg hydrogels rely on the versatility of dopamine, which may form structures for protection, self-healing, encapsulation, controlled release or bio-sensing. The coupling of a pyro-catechol violet dye into the dopa-Alg hydrogel served as a pH indicator with reversible color change and good stability provided by confinement into the gel [168]. Due to hydrogen bonding with catechol hydroxyl groups, the chemical stability of the colorimetric dye under a variety of pH conditions or in corrosive environment was improved, together with better mechanical stability after internal crosslinking. Alternatively, the release properties could be regulated in presence of magnetite particles (**Figure 15**), providing a medium for simultaneous crosslinking and magnetically-stimulated release [169]. The loading efficiency of active ingredients highly depends on the porosity of the hydrogel, while the release was chemically controlled by weakening of the electrostatic interactions after hydration of the dopa- protonated amino groups and the Alg-carboxylate groups. The self-healing characteristics and water-retention of dopa-Alg hydrogels were mastered through the Fe^{3+} coordination of the polymer network in relation with the pH-dependent degree of crosslinking [170], resulting in a progressively softer gel at low pH. The softness was further enhanced by charging and repulsive forces between adjacent polymer chains. The pH dependent recovery and self-healing properties of dopa-Alg hydrogels

are mediated by the amount of hydrogen bridging and π - π stacking, and can indeed be proven by a reversible transition in the sol-gel characteristics upon rheological testing [171]. A better control over the balance between adhesion and self-healing properties can be obtained in a double crosslinked dopa-Alg hydrogel. The incorporation of poly(glutamic acid) for adhesion and catechol for oxidative crosslinking allowed for a better control of the gelation time. As such, the processing of Alg-hydrogels for biomedical purpose improved through the possibility for in-situ injection and curing.

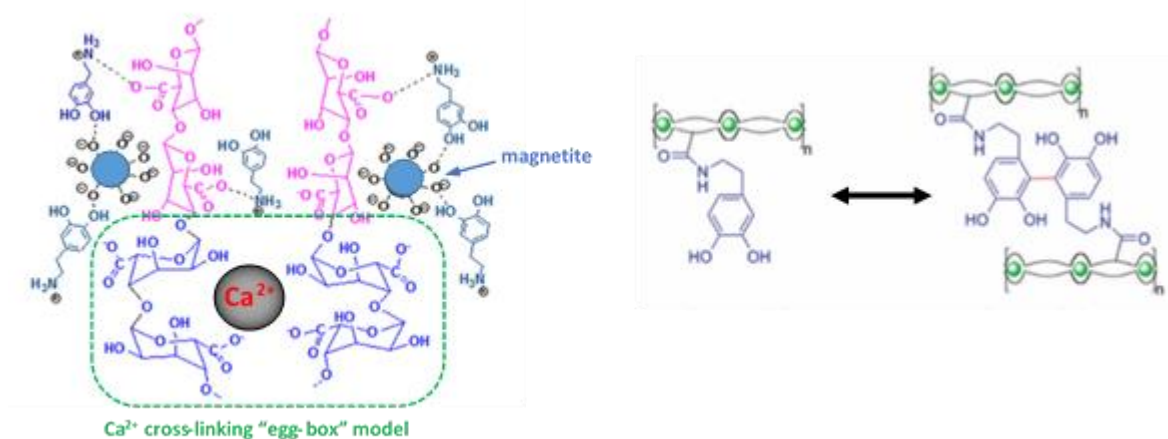


Figure 15. Functional properties of an Alg-hydrogel with additional features of controlled release through magnetic stimulation mediated by the addition of magnetite nanoparticles [169] ©2016 with permission from Elsevier.

For biomedical applications, the dopa-Alg surgery membranes were fabricated by freeze-drying of a modified hydrogel and show strong bio-adhesion in both *in-vitro* and *in-vivo* tests [172]. The adhesion of dopa-Alg with tissue in wet conditions or in presence of body fluids was mediated by the covalent bonding between oxidized quinone groups with amino-, hydroxyl, or thiol groups present in the tissue proteins. However, a reduction in mechanical properties was noticed after crosslinking of dopa-Alg with calcium ions during gelation, as the dopamine may interfere with the self-organization and interchain configuration in presence of calcium. Therefore, the derivatization of dopamine with chemo-enzymatic groups was proposed to enhance the gel formation in presence of calcium [173]. On the other hand, more robust free-standing Alg membranes for surgery with appropriate mechanical properties were created by crosslinking without calcium [174]. The dopamine sites themselves served as crosslinking medium where mostly covalent aryl-aryl coupling took place between the dopa-Alg and PDA aggregates. The modified surgery membranes could be provided with asymmetric composition depending on the organization of hydrophilic dopa-sites at the air/water interface. As such, the surgery membranes of dopa-Alg gained selective adhesion and adsorption properties at both sides of the material.

7. GENERAL CATECHOL MODIFICATION OF POLYSACCHARIDE MATERIALS

Besides dopamine, other natural polyphenols for functionalization of polysaccharides may originate from extracts of plants, tea, chocolate, wine. Particular examples applied for cellulose surface modification are tannic acid, gallic acid, hydroxyl-benzoic acid or caffeic acid. The main phenolic components of essential oils such as carvacrol, eugenol or thymol have hydroxyl groups and are acidic in nature, therefore presenting high activity against bacteria (**Figure 16**). The interaction between polysaccharides and catechols can additionally be mediated through enzymatic control with laccase. The laccase is particularly reactive towards aromatic groups and easily couples to lignocelluloses. The laccase treatment of lignin creates multiple phenoxy radicals that become available for mutual crosslinking. Thus, the residual surface lignin onto cellulose pulp fibers may provide a good medium for functionalization by surface grafting of the aromatic groups. It is known that also other biological enzymes such as tyrosinase act as a catalyst for the oxidation of dopa and related catechol(amines) [175]. Contrarily, the cellulose nanomaterials were used as an immobilization matrix for laccase-mediated deposition of silver nanoparticles or polyaniline, which served as a biosensor for the detection of catechol [176, 177].

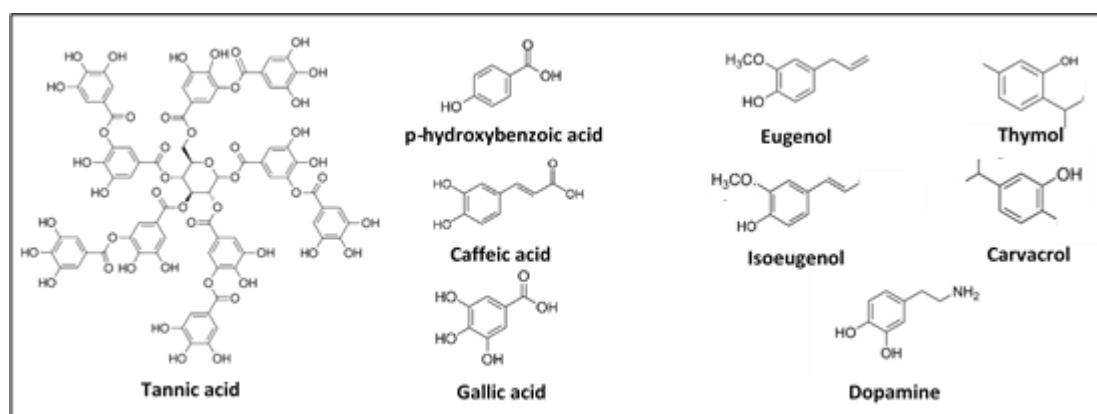


Figure 16. Chemical structure of alternative polyphenolic acids or extracts.

7.1 Tannic acid

Tannic acid (TA) is a natural polyphenol with high density of pyrogallol and catechol groups, which is obtained as a derivative of tannin and is commercially available as a plant extract. Although the mechanisms for modification and adhesion of tannin and dopamine are similarly based on polyphenol chemistry, the TA is less expensive, provides stronger adhesion and faster deposition rates. Whereas the dopamine crosslinking by oxidative polymerization or coordination bonding requires basic pH conditions, the adhesive properties simultaneously decrease by a drastic reduction in hydrogen bonding of the catechol. Therefore, the conditions leading to high cohesive and adhesive strength of dopamine

are in conflict [178]. In natural systems for mussel adhesion, the weakening of adhesiveness due to catechol oxidation is balanced in a much more complex system: a local environment free of seawater and with high acidity is created during secretion of *Mefp*, in order to ensure strong adhesion of *Mefp-3* and *Mefp-5* [179], together with suppressing the adverse effects of catechol oxidation by adopting thiol-rich *Mefp-6* as a reducing agent [180].

In contrast with dopamine, the TA serves as an efficient crosslinker under acidic conditions through various mechanisms such as hydrogen bonding, ionic bonding, coordination bonding to several metal ions (Fe, V, Cu, Ni, Mg, Zn), and hydrophobic interactions between the catechol and gallol groups. However, the complexation of TA with metal ions is most efficient at neutral pH to avoid protonation of the catechol groups. As such, the high cohesive and adhesive strength is combined in presence of pyrogallol/catechol groups and the dendritic structure of TA. The TA possesses also high reactivity towards thiol and amine monomers for surface attachment and reductant properties. Therefore, the TA acts as an interesting intermediate layer for surface modification through co-deposition of multiple layers under low pH. The main purposes of TA functionalization for polysaccharides focus on the formulation of nanocomposites and/or hydrogels. For biomedical applications such as wound dressing or medical devices, the TA specifically inhibits the growth of microbial biofilms and reduces the risk of infections in the human body. The antibacterial properties of TA are mainly attributed to the interruption of communication signals between bacteria which are associated with the intercellular adhesion of bacteria. The deposition of active groups on TA-cellulose as a ligand for further functionalization has been applied for the production of cellulose filtration membranes with enhanced antimicrobial properties and selective adsorption, as detailed below.

The functionalization of cellulose with TA can be done by non-covalent binding, while it converts into covalent bonds of the catechol after crosslinking [181]. The binding mechanism of TA polyphenols is similar to catechols and happens through oxidative reactions with formation of instable intermediates such as quinones, which bind to cellulose by covalent coupling [182], or hydrogen bonding and π - π stacking [183]. The deposition of TA on cellulose may directly happen under oxidizing conditions through quinone intermediates [184]. Alternatively, the oligomerization of polyphenolic TA in presence of oxygen leads to the formation of higher molecular weight species, which have lower solubility and spontaneously precipitate as a coating on cellulose [185]. The functionalization of viscose fibers with TA provided a medium for the in-situ reduction of silver nanoparticles from silver salt solution. After immobilization on antibacterial textiles, robust adhesion was provided after several washing cycles due to the strong chelation with multiple catechols [186]. The deposition of Ag can be optimized during serial deposition of alternating layers with TA and Ag, in order to make the coating more dense and prevent leaching of the nanoparticles [187]. In presence of TA, the nanoparticle shapes are more homogeneous without cluster formation and the distribution over the fiber surface becomes more uniform to retain a porous structure. The alternation of chitosan and TA layers onto electrospun fiber

mats of cellulose acetate also demonstrates enhanced mechanical and anti-microbial properties [188]. Under acid pH conditions, the TA is negatively charged due to protonation of the phenolic hydroxyl groups, which is suitable for self-assembly of the multilayers and restricts swelling of the electrospun cellulose fibers. In addition, the combination of TA and decylamine favourably provides a route for hydrophobic surface modification [189]. The attachment of hydrophobes onto a TA interlayer may happen through covalent coupling between the amino moieties and quinone groups of oxidized TA.

The cellulose nanocrystals of TA-CNC were used as carriers for active binding and loading of hydrophobic moieties or pharmaceuticals with relatively higher concentrations and retention efficiency than pure CNC [190]. The TA-CNC was also frequently added as a mechanical reinforcement and/or barrier material in composite materials, as demonstrated for chitosan films [191]. The stability of the chitosan polymer network initially increased through hydrogen bonding of TA-CNC and mechanical strength further increased after thermal crosslinking of TA.

The cellulose nanofibrils of TA-CNF allowed to construct mechanically robust nanocomposites by mimicking the nacre-structure: e.g., a layered structure with interconnections of graphene nanosheets and CNF was mediated by a TA interlayer and provides a composite material with anisotropic thermal and electrical conductivity [192]. The TEMPO-oxidized CNF favourably induced self-polymerization of TA as an adherent interlayer with reduced graphite oxide nanosheets, providing enhanced dispersion, exfoliation and anchoring of the nanosheets within the CNF template structure [193]. As such, the presence of TA allowed to obtain the simultaneous surface functionalization and reduction of graphite oxide during polymerization, while the nanohybrid complex could be further incorporated into a soy protein matrix (**Figure 17a**). After conversion of a TA-CNF network into a composite hydrogel, a micro-porous medium was created with additional features such as rapid self-healing, stretching, moulding, antioxidant and antibacterial properties [194]. The presence of TA significantly affects the visco-elastic properties of the hydrogel through the formation of a double crosslinked network with permanent bonding between the different hydrogens and dynamic ester bonding with the PVA matrix. The resulting hydrogel maintained good flow properties together with high ductility after crosslinking. The mechanical and self-healing properties were highly manipulated in presence of TA-CNF, where the reinforcing phase of CNF resulted in a remarkable improvement in tensile strength and stability, whereas the TA made the hydrogel softer and highly stretchable. The subsequent freeze-drying of TA-CNF suspensions resulted in the formation of aerogels with more homogeneous microporosity [195]. The TA-CNF could be subsequently functionalized with siloxanes through hydrolyzation/condensation reactions with the multi-aromatic structure of TA, introducing hydrophobic properties that depend on the length of alkyl chains of the organoalkoxysiloxane (**Figure 17b**). The active TA sites are able to render oil/water separation and simultaneously serve as anchoring points for capturing metal ions or organic pollutants. The microporous structures with controlled release were also obtained from modified bacterial cellulose (TA-BC), where reversible bonding between BC and TA is controlled through Mg^{2+}

crosslinking (**Figure 17c**) [196]. The ionic bonding of TA to Mg^{2+} and hydrogen interaction between the catechol and BC is regulated by the operational pH, as the catechol moieties become more protonated under acid environment. As such, the crosslink density and release profile of TA-BC can be steered by the Mg^{2+} concentration, providing efficient media for medicinal drug supply or TA supply as anti-microbial agent.

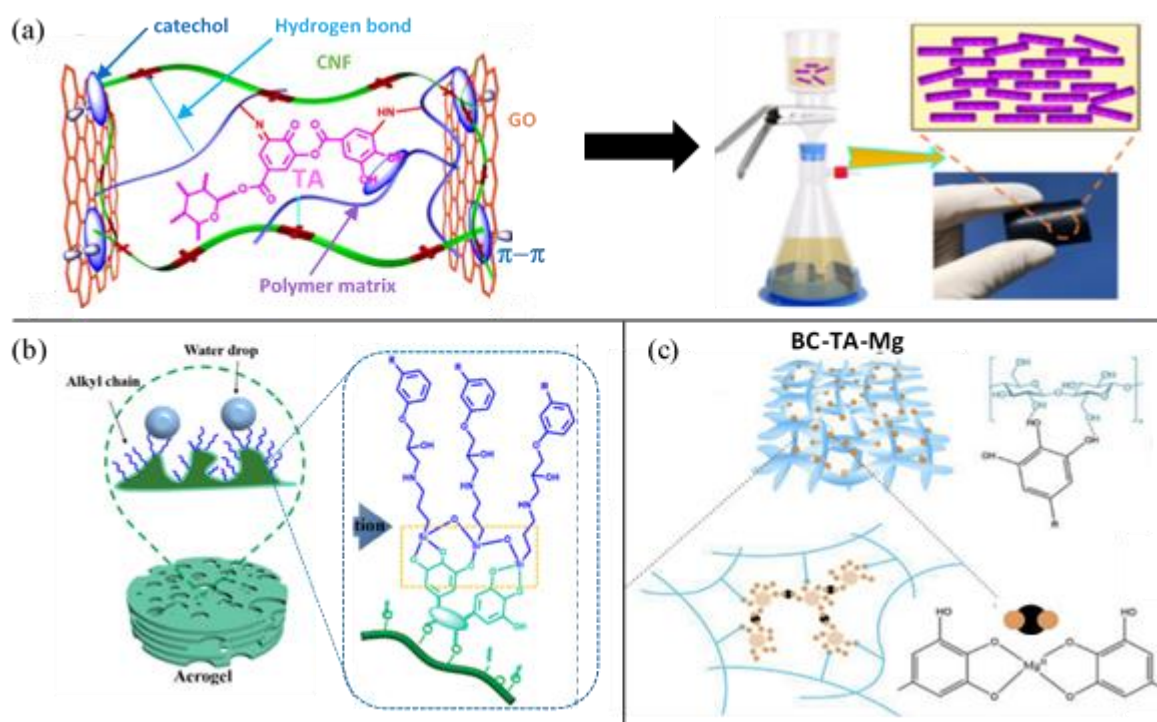


Figure 17. TA modification of nanocelluloses and incorporation of functional properties, (a) TA-CNF combined with graphene-oxide (GO) nanosheets and incorporation in polymer nanocomposite [193] ©2018 with permission from Elsevier, (b) TA-CNF aerogel with hydrophobic properties through organoalkoxysiloxane and TA interlayer [195] ©2020 with permission from Elsevier, (c) TA-BC composites with reversible bonding through Mg^{2+} complexation for release of TA as anti-microbial agent [196] ©2020 with permission from Elsevier.

7.2 Caffeic acid

The hydroxycinnamic or caffeic acid (CA) contains a molecular structure with phenolic and acrylic groups, occurring in nature as an intermediate in the lignin biosynthesis. The conjugation of CA with polysaccharides was demonstrated in the formulation of CA-chitosan hydrogels [197]. The grafting of CA to chitosan happened under acid conditions, using carbodiimide chemistry: at a critical concentration of 10 wt.-% CA, the CA-chitosan coating forms on magnetite nanocrystals resulting in better water-solubility and monodisperse particle sizes [198], while aggregation occurs at higher concentrations of CA

[199]. The CA-chitosan exhibits favourable solubility depending on pH conditions, in contrast with precipitation of unmodified chitosan at $\text{pH} > 2$. The gel-like properties of CA-chitosan at $\text{pH} > 8$ are triggered by chemical crosslinking upon oxidation of the catechol. The favourable suppression of oxidation and availability of non-oxidized CA at low pH conditions is required to enhance the adhesion, in contrast with the oxidation at higher pH leading to the formation of catechol-quinone intermediates and inter-/intramolecular amide adducts. Besides the good balance of adhesive and cohesive properties, the CA-chitosan was employed as biomedical materials with mucoadhesive properties [200], as bio-inks during complexation with serum proteins and metal ions [201], or in combination with reduced graphene oxide and platinum nanoparticles for biosensing [202].

7.3 Laccase-mediated catechol functionalization

The laccase is a catalytic enzyme of oxido-reductases with copper and it occurs in nature to promote the formation of lignin by oxidative polymerization of monolignols through subsequent radical reactions. Therefore, laccase can be used as a novel bio-catalyst for polymerization, crosslinking and functionalization of aromatic groups, phenols and aniline. In particular, modification of unbleached kraft pulp fibers with catechols was favourably done in presence of laccase, which preferentially induced covalent bonding with residual lignin on the fiber surface [203]. The oxidative transformation of aromatics involves the creation of a free cation radical after the transfer of a single electron to laccase, followed by the further radical reaction by non-enzymatic oxidation into dimers, oligomers and polymer molecules. Recent studies on the polymerization kinetics suggested that the laccase-assisted oxidation of catechols also proceeds through a mechanism of nucleophilic attack [204]. In presence of laccase, the coating of cellulose with catechols happens by enzymatic polymerization under low temperature, low water consumption and intermediate pH in order to preserve the fiber structure.

The modification of cellulose pulp fibers with a primary laccase layer was employed as an alternative route to coat cellulose fibers with polycatechols (**Figure 18a**): the cellulose fibers were first grafted with amine-functional groups and subsequently modified through the coupling with polycatechol [205]. The use of a laccase interlayer favoured the simultaneous oxidative polymerization of catechol and coupling to amines at the cellulose surface. The coupling reaction of the polycatechol in presence of laccase may be controlled through the preferential formation of mono- and di-amine quinone bonding resulting in the deposition on amine-cellulose, rather than the self-coupling of catechol or aromatic amines. The chemical stability of the modified cellulose fibers against enzymatic degradation and hydrolysis with cellulase is significantly enhanced, as the polycatechol layer provides steric hindrance to the cellulase and the specific crystalline binding domains for degradation of cellulose are blocked. As such, the enzymatic laccase modification of cellulose allows for smoother processing and higher quality.

The immobilization of laccase on bacterial cellulose (BC) allows to create active interaction sites for enzymatic reactions and was enhanced for dopa-BC. The grafting of laccase to BC is a very mild overnight process at room temperature with high retention of its initial activity. Alternatively, the deposition of PDA nanoparticles on dopa-BC formed preferential spots for covalent bonding of laccase (**Figure 18b**) [206]. The immobilized laccase has higher thermal stability than free laccase due to a restrained molecular mobility and ionic or covalent bonding. In contrast to dopa-CNC or dopa-CNF, the crystallinity of dopa-BC decreased during self-polymerization of PDA in presence of laccase. This is likely due to swelling of the BC fibers, as the primary hydroxyl groups in highly crystalline *I α* cellulose are preferentially oxidised under alkali treatment [207]. The deposition of laccase on BC filtration membranes may enhance the removal efficiency of organic dyes and provides anti-microbial properties.

The bacterial cellulose (BC) with functional laccase sites served as a catalytic platform for the fixation of catechol flavonoids [208]. The selection of specific catechols or phenols allows for a color change upon oxidation by immobilized laccase. The colour of catechol oligomers is due to the formation of π -conjugates and depends on the polymerization conditions: the light colours appear in presence of soluble polymers under mild oxidation, while dark colours appear after the formation of insoluble precipitates under strong oxidation. The laccase-mediated coloration was further elaborated through a better control of the enzymatic oxidation of catechols in a high-pressure homogenizer [209]: the reaction times were shortened and a higher degree of oligomerization was obtained with nanometer-size catechol particles that were more favourable for coloration. The methods for laccase immobilization can also be applied for the catalysed polymerization of other phenolics (e.g., catechol, hydroquinone, catechin, ferulic acid) and are a novel route for a clean and bio-based coloration of textiles.

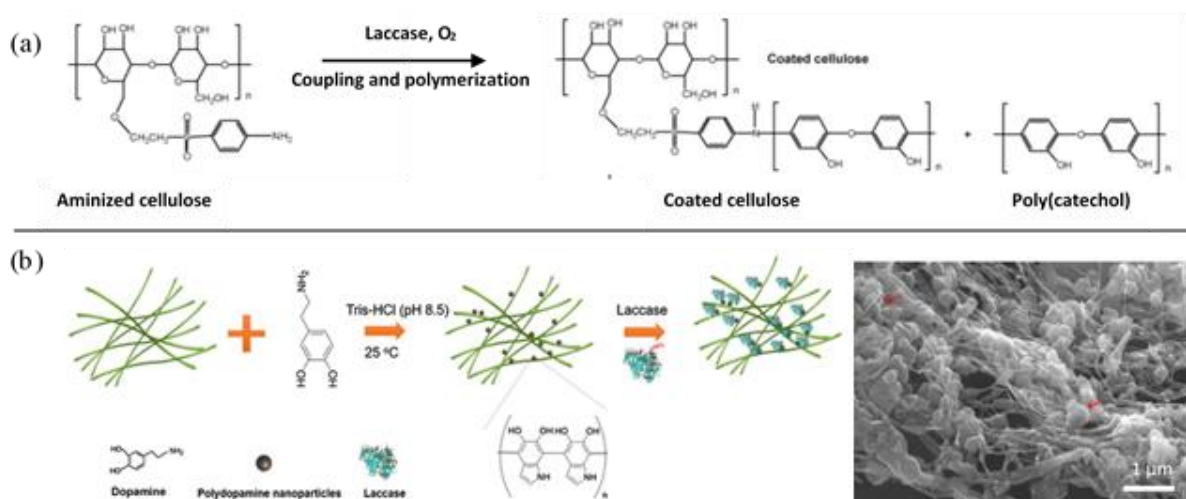


Figure 18. Enzymatic functionalization of cellulose with laccase in presence of dopamine, (a) enzymatic laccase-mediated polymerization for surface functionalization of cellulose materials [205], (b) dopa-BC scaffold membranes used for the immobilization of laccase as a support for controlling enzymatic reactions [206] ©2019 with permission from Springer Nature, (b) ©2007 with permission from Elsevier.

8. CONCLUSION AND OUTLOOK

According to state-of-the art literature, the polydopamine (PDA) and polysaccharides (i.e., cellulose, chitin/chitosan, alginate) show excellent interactions as biological macromolecules and offer plenty of opportunities to create innovative functionalized materials under mild chemical reaction conditions. Approaches and applications can be applied for the modification of cellulose, chitin/chitosan or alginate and their respective nanomaterials.

The self-polymerization of a PDA layer under oxidative conditions with formation of intermediate quinone allows for simultaneous covalent binding with polysaccharide surfaces, through chemical grafting following Schiff-base amination or Michael addition reaction, and/or by carbodiimide coupling chemistry. The alternative interaction mechanisms evidently occur through hydrogen bonding of the catechol and in-situ reduction of metal ions. Besides presence of hydroxyl groups at cellulose surfaces, the amine functional groups on chitin surfaces are available for direct chemical binding. The modified polysaccharides can be stabilized through enhanced crosslinking reactions towards a defined degree of network formation due to coordination bonds of metal chelation complexes. The latter evidently improve the thermal stability or mechanical properties and reduce swelling of the material. However, the strict control on reaction conditions for surface modification is crucial, in particular the pH determining the oxidation state of the catechol/quinone groups, the eventual formation of catechol adducts and direct interactions with the amino surface groups in chitosan.

The PDA allows to introduce multiple properties either as a surface layer for tuning adhesive and crosslinking properties, either as an intermediate reactive layer to enable further interaction with polymer and/or metallic components. As such, the functionality of the modified polysaccharides can be tuned towards desired performance with, e.g., mechanical reinforcement, (super-)hydrophobicity or wettability, anti-microbial properties, photocatalytic activity, electrical and thermal conductivity, fire resistance, biocompatibility and -adhesion, self-healing, sensing and responsive ability, selective adsorption, controlled release. Therefore, the materials gained interest in technical applications including bio-based (nano)composites, textiles, hydrogels, adhesives, membranes for filters or scaffolds, films, energy devices, aerogels and hydrogels.

In future, the scientific field would benefit from an integrated approach and valorization of the entire mussel-inspired adhesive mechanism. Novel approaches should consider bio-mimicking of the entire adhesive system, rather than purely focussing on the catechol moieties. The additional contributions of, e.g. lysine, cysteine, tyrosine residues were not yet sufficiently understood and considered in augmenting the performance of synthetic systems. In addition, the intrinsic self-regulation of suitable biological environments is difficult to fully implement in synthetic analogues, while it may both increase the performance in specific cases and/or restrict the general applicability. Also, the present routes for extraction of mussel foot proteins are not yet viable at industrial scale. Therefore, the exploitation of

favourable features of dopamine currently requires the incorporation of adhesive functionalities in synthetic polymers. Hopefully, also the efficiency of other natural polyphenolics have been considered as alternatives. The present state-of-art is a result from the highly interdisciplinary work between biologists, chemists and materials scientists and should remain focussing on the further integration of additional biotechnological resources and industrial up-scaling. This will remain a key drive in the future development of sustainable and innovative materials.

References.

1. Von Byern, J., Klepal, W. Adhesive mechanisms in cephalopods: a review. *Biofouling* **2006**, *22*, 329-338.
2. Malshe, A.P., Bapat, S., Rajurkar, K.P., Haitjema, H. Bio-inspired textures for functional applications. *CIRP Annals* **2018**, *67*, 627-650.
3. Liu, M., Zheng, Y. and Jiang, L. Bioinspired super-antiwetting interfaces with special liquid-solid adhesion. *Acc. Chem. Res.* **2010**, *43*, 368-377.
4. Li, Y., Krahn, J., Menon, C. Bioinspired dry adhesive materials and their application in robotics: a review. *J. Bionic Eng.* **2016**, *13*, 181-199.
5. Ma, S., Wu, Y., Zhou, F. Bio-inspired synthetic wet adhesives: from permanent bonding to reversible regulation. *Curr. Opin. Colloid Interfac. Sci.* **2020**, *47*, 84-94.
6. Zhao, Y., Wu, Y., Wang, L., Zhang, M., Chen, X., Liu, M., Liu, F., Zhou, F., Wang, Z. Bio-inspired reversible underwater adhesive. *Nature Commun.* **2017**, *8*, 2218.
7. Wunderer, J., Lengerer, B., Pjeta, R., Bertemes, P., Kremser, L., Lindner, H., Ederth, T., Hess, M.W., Stock, D., Salvenmoser, W., Ladurner, P. A mechanism for temporary bioadhesion. *PNAS* **2019**, *116*, 4297-4306.
8. Autumn, K. Gecko adhesion: structure, function, and applications. *MRS Bulletin* **2007**, *32*, 473-478.
9. Li, J., Liu, J., Ma, C., Ji, J., and Liu, J., Mechanisms underlying the biological wet adhesion: coupled effects of interstitial liquid and contact geometry. *J. Bionic Eng.* **2020**, *17*, 448-456.
10. Morales-Garcia, A.L., Bailey, R.G., Jana, S., Burgess, J.G. The role of polymers in cross-kingdom bioadhesion. *Phil. Trans. R. Soc. London B Biol. Sci.* **2019**, *374*, 20190192.
11. Schmidgall, J., Schnetz, E., Hensel, A. Evidence for bioadhesive effects of polysaccharides and polysaccharide-containing herbs in an ex vivo bioadhesion assay on buccal membranes. *Planta Medica* **2000**, *66*, 48-53.
12. Yang, J., Keijsers, J., Heek, M., Stuijver, A., Cohen, S., Kamperman, M.M.G. The effect of molecular composition and crosslinking on adhesion of a bio-inspired adhesive. *Polymer Chemistry* **2015**, *6*, 3121-3130.
13. Brubaker, C.E., Messersmith, P.B., The present and future of biologically inspired adhesive interfaces and materials. *Langmuir* **2012**, *28*, 2200-2205.
14. Favi, P.M., Yi, S., Lenaghan, S.C., Xia, L., Zhang, M. Inspiration from the natural world: from bio-adhesives to bio-inspired Adhesives. *J. Adhes. Sci. Technol.* **2018**, *28*, 290-319.
15. Andersen, A., Chen, Y., Birkedal, H. bioinspired metal-polyphenol materials: self-healing and beyond. *Biomimetics* **2019**, *4*, 30.
16. Gardner, D.J., Oporto, G.S., Mills, R., Samir, A.S. Adhesion and surface issues in cellulose and nanocellulose. *J. Adhes. Sci. Technol.* **2008**, *22*, 545-567.
17. Berglund, J., Mikkelsen, D., Flanagan, B.M., Dhital, S., Gaunitz, S., Henrikson, G., Lindstrom, M.E., Yakubov, G.E., Gidley, M.J., Vilaplana, F. Wood hemicelluloses exert distinct biomechanical contributions to cellulose fibrillar networks. *Nature Commun.* **2020**, *11*, 4692.
18. Aldred, N., Chan, V.B., Emami, K., Okano, K., Clare, A.S., Mount, A.S. Chitin is a functional component of the larval adhesive of barnacles. *Commun. Biol.* **2020**, *3*, 31.
19. Rudall, K.M. Chitin and its association with other molecules. *J. Polym. Sci. C* **1969**, *28*, 83-102.
20. Ruiz-Herrera, J., Elorza, M.V., Valentin, E., Sentandrey, R. Molecular organization of the cell wall of *Candida albicans* and its relation to pathogenicity. *FEMS Yeast Res.* **2006**, *6*, 14-29.
21. Helfricht, N., Doblhofer, E., Biebern V., Lommès, P., Sieber, V., Scheibel, T., Papastavrou, G. Probing the adhesion properties of alginate hydrogels: a new approach towards the preparation of soft colloidal probes for direct force measurements. *Soft Matter* **2017**, *13*, 578-589.

22. Missoum, K., Belgacem, M.N., Bras, J. Nanofibrillated cellulose surface modification: a review. *Materials* **2013**, 6, 1745-1766.
23. Ifuku, S. Chitin and chitosan nanofibers: preparation and chemical modifications. *Molecules* **2014**, 19, 18367-18380.
24. Yang, J.S., Xie, Y.J., He, W. Research progress on chemical modification of alginate: a review. *Carbohydr. Polym.* **2011**, 84, 33-39.
25. Griffiths, C. L.; King, J. A. Energy expended on growth and gonad output in the ribbed mussel. *Mar. Biol.* **1979**, 53, 217-222.
26. Hawkins, A.J.S.; Bayne, B.L. Seasonal variation in the relative utilization of carbon and nitrogen by the mussel *Mytilus edulis*: budgets, conversion efficiencies and maintenance Requirements. *Mar. Ecol. Prog. Ser.* **1985**, 25, 181-188.
27. Lin, Q.; Gourdon, D.; Sun, C.J.; Holten-Andersen, N.; Anderson, T.H. Adhesion mechanisms of the mussel foot proteins mfp-1 and mfp-3. *Proc. Natl. Acad. Sci.* **2007**, 104, 3782-3786.
28. Lee, B.P.; Messersmith, P.B.; Israelachvili, J.N.; Waite, J.H. Mussel-inspired adhesives and coatings. *Annual Rev. Mater. Res.* **2011**, 41, 99-132.
29. Loizou, E.; Weisser, J.T.; Dundigalla, A.; Porcar, L.; Schmidt, G.; Wilker, J.J. Structural effects of crosslinking a biopolymer hydrogel derived from marine mussel adhesive protein. *Macromol. Biosci.* **2006**, 6, 711-718.
30. Guo, Q.; Chen, J.; Wang, J.; Zeng, H.; Yu, J. Recent progress in synthesis and application of mussel-inspired adhesives. *Nanoscale* **2020**, 12, 1307-1324.
31. Suci, P.A.; Geesy, G.G. Comparison of adsorption behavior of two mytilus edulis foot proteins on three surfaces. *Coll. Surf.B* **2001**, 22, 159-168.
32. Shin, M.; Shin, J.Y.; Kim, K.; Yang, B.; Han, J.W.; Kim, N.K.; Cha, H.J. The position of lysine controls the catechol-mediated surface adhesion and cohesion in underwater mussel adhesion. *J. Coll. Interfac. Sci.* **2020**, 536, 168-176.
33. Maier, G.P.; Rapp, M.; Waite, J.H.; Israelachvili, J.N.; Butler, A. Adaptive synergy between catechol and lysine promotes wet adhesion by surface salt displacement. *Science* **2015**, 349, 628-632.
34. Priemel, T.; Degtyar, E.; Dean, M.N.; Harrington, M.J. Rapid self-assembly of complex biomolecular architectures during mussel byssus biofabrication. *Nat. Commun.* **2017**, 8, 14539.
35. Waite, J.H. Mussel adhesion - essential footwork. *J. Exp. Biol.* **2017**, 220, 517-530.
36. Qin, Z.; Buehler, M.J. Molecular mechanics of mussel adhesion proteins. *J. Mech. Phys. Sol.* **2014**, 62, 19-30.
37. Sever, M.J.; Weisser, J.T.; Monahan, J.; Srinivasan, S.; Wilker, J.J. Metal-mediated crosslinking in the generation of a marine-mussel adhesive. *Agew. Chem.* **2004**, 43, 447-450s.
38. Yang, B.; Lim, C.; Hwang, D.S.; Cha, H.J. Switch of surface adhesion to cohesion by Dopa-Fe³⁺ complexation in response to the microenvironment at the mussel plaque/substrate interface. *Chem. Mater.* **2016**, 28, 7982-7989.
39. Zhang, W.; Yang, H.; Liu, F.; Chen, T.; Hu, G.; Guo, D.; Hou, Q.; Wu, X.; Su, Y.; Wang, J. Molecular interactions between DOPA and surfaces with different functional groups: a chemical force microscopy study. *RSC Adv.* **2017**, 7, 32518-32527.
40. Lee, H.; Scherer, N.F.; Messersmith, P.B. Single-molecule mechanics of mussel adhesion. *Proc. Nat. Acad. Sci.* **2006**, 103, 12999-13003.
41. Nicklisch, S.; Waite, J.H. Mini-review: The role of redox in DOPA-mediated marine adhesion. *Biofouling* **2012**, 28, 865-877.
42. Min, K.; Park, K.; Park, D.H.; Yoo, Y.J. Overview on the Biotechnological Production of L-DOPA, *Appl. Microbiol. Biotechnol.* **2014**, 99, 575-584.

43. Moulay, S. Recent trends in mussel-inspired catechol-containing polymers. *Orient. J. Chem.* **2018**, 34, 1153-1197.
44. Castillo, J.J.; B.K. Shanbheng, B.K.; He, L. Comparison of natural extraction and recombinant mussel adhesive proteins approaches, In: Puri M. (eds). *Food Bioactives*, **2017**, 111-135.
45. Strausberg, R.L.; Link, R.P. Protein-based medical adhesives. *Trends Biotechnol.* **1990**, 8, 53-57.
46. Hwang, D.S.; Yoo, H.J.; Jun, J.H.; Moon, W.K.; Cha, H.J. Expression of Functional Recombinant Mussel Adhesive Protein Mgfp-5 in Escherichia Coli. *Appl. Environ. Microbiol* **2004**, 70, 3352-3359.
47. Zhao, H.; Waite, J.H. Linking adhesive and structural proteins in the attachment plaque of *M. Californianus*. *J. Biol. Chem.* **2006**, 281, 26150-26158.
48. Taylor, S.W. Chemoenzymatic synthesis of peptidyl 3,4-dihydroxyphenylalanine for structure–activity relationships in marine invertebrate polypeptides. *Anal. Biochem.* **2002**, 302, 70-74.
49. Axambayeva, A.S.; Shagyrova, Z.; Nurgozhin, T.S.; Zhienbay, E.; Shustov, A.V. Novel material: biocompatible glue for use in biology and medicine—recombinant mussel adhesive proteins. *Eurasian J. Appl. Biotechnol.* **2016**, 3.
50. Bilotto, P.; Labate, C.; De Santo, M.P.; Deepnankumar, K.; Miserez, A.; Zappone, B. Adhesive properties of adsorbed layers of two recombinant mussel foot proteins with different levels of dopa and tyrosine. *Langmuir* **2019**, 25, 15481-15490.
51. Hwang, D.S.; Yoo, H.J.; Jun, J.H.; Moon, W.K.; H.J. Cha, H.J. Expression of functional recombinant mussel adhesive protein Mgfp-5 in Escherichia coli. *Appl. Environ. Microbiol.* **2004**, 70, 3352-3359.
52. Hwang, D.S.; Gim, Y.; Yoo, H.J.; Cha, H.J. Practical recombinant hybrid mussel bioadhesive. *Biomaterials* **2007**, 28, 3560-3568.
53. Wang, J.; Scheibel, T. Recombinant Production of Mussel Byssus Inspired Proteins. *Biotechnology Journal* **2018**, 13, 1800146.
54. Sever, M.J.; Wilker, J.J. Synthesis of peptides containing DOPA (3,4-dihydroxyphenylalanine). *Tetrahedron Lett.* **2001**, 57, 6139-6146.
55. Liu, Z.; Hu, B.H.; Messersmith, P.B. Convenient synthesis of acetonide protected 3,4-dihydroxyphenylalanine (DOPA) for Fmoc solid-phase peptide synthesis. *Tetrahedron Lett.* **2008**, 49, 5519-5521.
56. Statz, A.R.; Meagher, R.J.; Barron, A.E.; Messersmith, P.B. New Peptidomimetic Polymers for Antifouling Surfaces. *J. Am. Chem. Soc.* **2005**, 127, 7972-7973.
57. Bernini, R.; Barontini, M.; Crisante, F.; Ginnasi, M.C.; Saladino, R. A novel and efficient synthesis of DOPA and DOPA peptides by oxidation of tyrosine residues with IBX. *Tetrahedron Lett.* **2009**, 50, 6519-6521.
58. Horsch, J.; Wilke, P.; Pretzler, M.; Seuss, M.; Melnyk, I.; Remmler, D.; Fery, A.; Rompel, A.; Börner, H.G. Polymerizing like mussels do: toward synthetic mussel foot proteins and resistant glues. *Angew. Chem. Int.* **2018**, 57, 15728-15732.
59. Das, S.; Martinez-Rodriguez, N.R.; Wei, W.; Waite, J.H.; Israelachvili, J.N. Peptide length and dopa determine iron-mediated cohesion of mussel foot proteins. *Adv. Funct. Mater.* **2015**, 25, 5840-5847.
60. Tu, R.S.; Tirrell, M. Bottom-up design of biomimetic assemblies. *Adv. Drug Del. Rev.* **2004**, 56, 1537-1563.
61. Dehsorkhi, A.; Castelletto, V.; Hamley, I.W. Self-assembling amphiphilic peptides. *J. Pept. Sci.* **2014**, 20, 453-467.
62. Samyn, P.; Rühle, J.; Biesalski, M. Polymerizable biomimetic vesicles with controlled local presentation of adhesive functional dopa groups. *Langmuir* **2010**, 26, 8573-8581.

63. Samyn, P.; Shroff, K.; Prucker, O.; Rhe, J.; Biesalski, M. Colorimetric sensing properties of catechol-functional polymerized vesicles in aqueous solution and at solid surfaces. *Coll. Surf. A* **2014**, 441, 242-254.
64. Samyn, P.; Shroff, K.; Prucker, O.; Rhe, J.; Biesalski, M. Fluorescent sensibility of microarrays through functionalized adhesive polydiacetylene vesicles. *Sens. Act. A* **2014**, 214, 45-57.
65. Forooshani, P.K.; Lee, B.P. Recent approaches in designing bioadhesive materials inspired by mussel adhesive protein. *J. Polym. Sci. A* **2016**, 55, 9-33.
66. Lee, H.; Lee, B.P.; Messersmith, P.B. A reversible wet/dry adhesive inspired by mussels and geckos. *Nature* **2007**, 448, 338-341.
67. Yu M.E.; Hwang, J.Y.; Deming, T.J. Role of L-3,4 dihydroxyphenylalanine in mussel adhesive proteins. *J. Am. Chem. Sci.* **1999**, 121, 5825-5826.
68. Guvendiren, M.; Messersmith, P.B.; Shull, K.R. Self-assembly and adhesion of dopa-modified methacrylic triblock hydrogels. *Biomacromolec.* **2008**, 9, 122-128.
69. Lee, B.P.; Chao, C.Y.; Nunalee, F.N.; Motan, E.; Shull, K.R.; Messersmith, P.B. Rapid gel formation and adhesion in photocurable and biodegradable block copolymers with high DOPA content. *Macromolec.* **2006**, 39, 1740-1748.
70. Zhang, H.; Zhao, T.; Newland, B.; Duffy, P.; Annaidh, A.N.; O’Cearbhaill, A.D.; Wang, W. On-demand and negative-thermo-swelling tissue adhesive based on highly branched ambivalent PEG–catechol copolymers. *J. Mater. Chem. B* **2015**, 31, 6420-6428.
71. Doraiswamy, A.; Dinu, C.; Cristescu, R.; Messersmith, P.B.; Chisholm, B.J.; Stafslie, S.J.; Chrisey, D.B.; Narayan, R.J. Matrix-assisted pulsed-laser evaporation of DOPA-modified poly(ethylene glycol) thin films. *J. Adhes. Sci. Technol.* **2007**, 13, 287-299.
72. Hvidt, S.; Jorgenson, E.B.; Brown, W.; Schillen, K. Micellization and Gelation of Aqueous Solutions of a Triblock Copolymer Studied by Rheological Techniques and Scanning Calorimetry. *J. Phys. Chem.* **1994**, 98, 12320-12328.
73. Burke, S.A.; Jones, M.R.; Lee, B.P.; Messersmith, B.P. Thermal gelation and tissue adhesion of biomimetic hydrogels. *Biomed. Mater.* **2007**, 2, 203-210.
74. Jennissen, H.P.; Laub, M. Development of an universal affinity fusion tag. *Materwiss. u. Werkstofftechn.* **2007**, 38, 1035-1039.
75. Samyn, P. Polydopamine and Cellulose: two biomaterials with excellent compatibility and applicability. *Polymer Rev.* **2020**, submitted.
76. Lin, J.; Yang, Z.; Hu, X.; Hong, G.; Zhang, S.; Song, W. The effect of alkali treatment on properties of dopamine modification of bamboo fiber/poly(lactic acid) composites. *Polymers* **2018**, 10, 403.
77. Fan, Q.; Han, G.; Cheng, W.; Tian, H.; Wang, D.; Xuan, L. Effect of intercalation structure of organo-modified montmorillonite/poly(lactic acid) on wheat straw fiber/poly(lactic acid) composites. *Polymers* **2018**, 10, 896.
78. Hong, G.; Meng, Y.; Yang, Z.; Cheng, H.; Zhang, S.; Song, W. Mussel-inspired polydopamine modification of bamboo fiber and its effect on the properties of bamboo fiber/polybutyl succinate composites. *Bioresources* **2017**, 12, 8419-8442.
79. Samyn, P. Engineering the cellulose fiber interface in a polymer composite by mussel-inspired adhesive nanoparticles with intrinsic stress-sensitive responsivity. *ACS Appl. Mater. Interfac.* **2020**, 25, 28819-28830.
80. Xu, H.; Shi, X.; Ma, H.; Lv, Y.; Zhang, L.; Mao, Z. The preparation and antibacterial effects of dopa-cotton/AgNPs. *Appl. Surf. Sci.* **2011**, 257, 6799-6803.
81. Yang, J.; Xu, H.; Zhang, L.; Zhong, Y.; Sui, X.; Mao, Z. Lasting superhydrophobicity and antibacterial activity of Cu nanoparticles immobilized on the surface of dopamine modified cotton fabrics. *Surf. Coat. Technol.* **2017**, 309, 149-154.

82. Xi, J.; Xiao, J.; Xiao, F.; Jin, Y.; Dong, Y.; Jing, F.; Wang, S. Mussel-inspired functionalization of cotton for nano-catalyst support and its application in a fixed-bed system with high performance. *Sci. Reports* **2016**, *6*, 21904.
83. Cheng, D.; He, M.; Ran, J.; Cai, G.; Wu, J.; Wang, X. In-situ reduction of TiO₂ nanoparticles on cotton fabrics through polydopamine templates for photocatalysis and UV protection. *Cellulose* **2018**, *25*, 1413-1424.
84. Fan, J.; Yu, D.; Wang, W.; Liu, B. The self-assembly and formation mechanism of regenerated cellulose films for photocatalytic degradation of C.I. reactive blue 19. *Cellulose* **2019**, *26*, 3955-3972.
85. Ran, J.; Bi, S.; Jiang, H.; Telegin, F.; Bai, X.; Yang, H.; Cheng, D.; Cai, G.; Wang, X. Core-shell BiVO₄@PDA composite photocatalysts on cotton fabrics for highly efficient photodegradation under visible light. *Cellulose* **2019**, *26*, 6259-6273.
86. Sadi, S.; Pan, J.; Xu, A.; Cheng, D.; Cai, G.; Wang, X. Direct dip-coating of carbon nanotubes onto polydopamine-templated cotton fabrics for wearable applications. *Cellulose* **2019**, *26*, 7569-7579.
87. Si, Y.; Guo, Z. Eco-friendly functionalized superhydrophobic recycled paper with enhanced flame-retardancy. *J. Colloid. Interfac. Sci.* **2016**, *477*, 74-82.
88. Qin, Z.; Liu, W.; Chen, H.; Chen, J.; Wang, H.; Song, Z. Preparing photocatalytic paper with improved catalytic activity by in-situ loading poly-dopamine on cellulose fibers. *Bull. Mater. Sci.* **2019**, *42*, 54 (6p).
89. Hollertz, R.; Duran, V.L.; Larsson, P.A.; Wagberg, L. Chemically modified cellulose micro- and nanofibrils as paper-strength additives. *Cellulose* **2017**, *24*, 3883-3899.
90. Wang, G.; Zhang, J.; Lin, S.; Xiao, H.; Yang, Q.; Chen, S.; Yan, B.; Gu, Y. Environmentally friendly nanocomposites based on cellulose nanocrystals and polydopamine for rapid removal of organic dyes in aqueous solution. *Cellulose* **2020**, *27*, 2085-2097.
91. Hu, D.; Huang, H.; Jiang, R.; Wang, N.; Xu, H.; Wang, Y.G.; Ouyang, X.K. Absorption of diclofenac sodium on bilayer amino-functionalized cellulose nanocrystals/chitosan composite. *J. Hazard Mater* **2019**, *369*, 483-493.
92. Liu, S.; Chen, Y.; Liu, C.; Gan, L.; Ma, X.; Huang, J. Polydopamine-coated cellulose nanocrystals as an active ingredient in poly(vinyl alcohol) films towards intensifying packaging application potential. *Cellulose* **2019**, *26*, 9599-9612.
93. Li, L.; Bao, R.Y.; Gao, T.; Liu, Z.Y.; Xie, B.H.; Yang, M.B.; Yang, W. Dopamine-induced functionalization of cellulose nanocrystals with polyethylene glycol towards poly(L-lactic acid) bionanocomposites for green packaging. *Carbohydr. Polym.* **2019**, *203*, 275-284.
94. Wang, G.; Zhang, J.; Lin, S.; Xiao, H.; Yang, Q.; Chen, S.; Yan, B.; Gu, Y. Environmentally friendly nanocomposites based on cellulose nanocrystals and polydopamine for rapid removal of organic dyes in aqueous solution. *Cellulose* **2020**, *27*, 2085-2097.
95. Tang, J.; Shi, Z.; Berry, R.M.; Tam, K.C. Mussel-inspired green metallization of silver nanoparticles on cellulose nanocrystals and their enhanced catalytic reduction of 4-nitrophenol in presence of cyclodextrin. *Ind. Eng. Chem. Res.* **2015**, *54*, 3299-3308.
96. Wu, X.; Shi, Z.; Fu, S.; Chen, J.; Berry, R.M.; Tam, K.C. Strategy for synthesizing porous cellulose nanocrystal supported metal nanocatalysts. *ACS Sus. Chem. Eng.* **2016**, *4*, 5929-5935.
97. Mirkovic, I.; Lei, L.; Ljubic, D.; Zhu, S. Crystal growth of metal-organic framework-5 around cellulose-based fibers having a necklace morphology. *ACS Omega* **2019**, *4*, 169-175.
98. Karabulut, E.; Pettersson, T.; Ankerfors, M.; Wagberg, L. Adhesive layer-by-layer films of carboxymethylated cellulose nanofibril-dopamine covalent bioconjugated inspired by marine mussel threads. *ACS Nano* **2012**, *6*, 4731-4739.

99. Liu, X.; Gu, W.; Wang, K.; Zhang, W.; Xia, C.; Shi, S.Q.; Li, J. Thiol-branched graphene oxide and polydopamine-induced nanofibrillated cellulose to strengthen protein-based nanocomposite films. *Cellulose* **2019**, *26*, 7223-7236.
100. Jin, S.; Li, K.; Gao, Q.; Zhang, W.; Chen, H.; Li, J. Development of conductive protein-based film reinforced by cellulose nanofibril template-directed hyperbranched copolymer. *Carbohydr. Polym.* **2020**, *237*, 116141.
101. Liu, Y.; Sui, Y.; Liu, C.; Liu, C.; Wu, M.; Li, B.; Li, Y. A physically crosslinked polydopamine/nanocellulose hydrogel as potential versatile vehicles for drug delivery and wound healing. *Carbohydr. Polym.* **2018**, *188*, 27-36.
102. Tang, J.; Song, Y.; Zhao, F.; Spinney, S.; Bernardes, J.; Tam, K.C. Compressible cellulose nanofibril (CNF) based aerogels produced via a bio-inspired strategy for heavy metal ion and dye removal. *Carbohydr. Polym.* **2019**, *208*, 404-412.
103. Li, Y.; Wang, B.; Sui, X.; Xu, H.; Zhang, L.; Zheng, Y.; Mao, Z. Facile synthesis of microfibrillated cellulose/organosilicon/polydopamine composite sponges with flame retardant properties. *Cellulose* **2017**, *24*, 3815-3823.
104. Feng, J.; Shi, Q.S.; Li, W.R.; Shu, X.I.; Chen, A.M.; Xie, X.B.; Huang, X.M. Antimicrobial activity of silver nanoparticles in situ growth on TEMPO-mediated oxidized bacterial cellulose. *Cellulose* **2014**, *21*, 4557-4567.
105. Sureshkumar, M.; Siswanto, D.Y.; Lee, C.K. Magnetic antimicrobial nanocomposite based on bacterial cellulose and silver nanoparticles. *J. Mater. Chem.* **2010**, *20*, 6948-6955.
106. Xie, Y.; Yue, L.; Zheng, Y.; Zhao, L.; Liang, C.; He, W.; Liu, Z.; Sun, Y.; Yang, Y. The antibacterial stability of poly(dopamine) in-situ reduction and chelation nano-Ag based on bacterial cellulose network template. *Appl. Surf. Sci.* **2019**, *491*, 383-394.
107. Lai, C.; Zhang, S.J.; Sheng, L.Y.; Xi, T.F. Comparative evaluation of the biocompatible and physical-chemical properties of poly(lactide-co-glycolide) and polydopamine as coating materials for bacterial cellulose. *J. Mater. Chem. B* **2019**, *7*, 630-639.
108. Khamrai, M.; Banerjee, S.L.; Paul, S.; Ghosh, A.K.; Sarkar, P.; Kundu, P.P. A mussel mimetic, bioadhesive, antimicrobial patch based on dopamine-modified bacterial cellulose/rGO/Ag NPs: A green approach toward wound-healing applications. *ACS Sus. Chem. Eng.* **2019**, *7*, 12083-12097.
109. Derami, H.G.; Jiang, Q.; Ghin, D.; Cao, S.; Chandar, Y.J.; Morrissey, J.J.; Jun, Y.S.; Singamaneni, S. A robust and scalable polydopamine/bacterial nanocellulose hybrid membrane for efficient wastewater treatment. *ACS Appl. Nano Mater.* **2019**, *2*, 1091-1101.
110. Ai, K.; Liu, Y.; Ruan, C.; Lu, L.; Lu, G. Sp² C-dominant N-doped carbon sub-micrometer spheres with a tunable size: a versatile platform for highly efficient oxygen-reduction catalysts. *Adv. Mater.* **2013**, *25*, 998-1003.
111. Au-Dong, A.; Lee, C.K. Flexible metal-organic framework-bacterial cellulose nanocomposite for iodine capture. *Cryst Growth Des* **2018**, *18*, 356-363.
112. Xie, Y.; Zheng, Y.; Fan, J.; Wang, Y.; Yue, L.; Zhang, N. Novel electronic-ionic hybrid conductive composites for multifunctional flexible bioelectrodes based on in situ synthesis of poly(dopamine) on bacterial cellulose. *Appl. Mater. Interface* **2018**, *10*, 22692-22702.
113. Jiang, Q.; Derami, H.G.; Ghim, D.; Cao, S.; Jun, Y.S.; Singamaneni, S. Polydopamine-filled bacterial nanocellulose as a biodegradable interfacial photothermal evaporator for highly efficient solar steam generation. *J. Mater. Chem. A* **2017**, *5*, 18397-18402.
114. Zhang, Z.J.; Chen, X.Y. Carbon nanofibers derived from bacterial cellulose: surface modification by polydopamine and the use of ferrous ion as electrolyte additive for collaboratively increasing the supercapacitor performance. *Appl. Surf. Sci.* **2020**, *519*, 146252.

115. Liang, H.W.; Wu, Z.Y.; Chen, L.F.; Li, C.; Yu, S.H. Bacterial cellulose derived nitrogen-doped carbon nanofiber aerogel: An efficient metal-free oxygen reduction electrocatalyst for zinc-air battery. *Nano Energy* **2015**, *11*, 366-376.
116. Luo, W.; Wang, B.; Heron, C.G.; Allen, M.J.; Morre, J.; Maier, C.S.; Stickle, W.F.; Ji, X. Pyrolysis of cellulose under ammonia leads to nitrogen-doped nanoporous carbon generated through methane formation. *Nano Lett.* **2014**, *14*, 2225-2229.
117. Hwang, D.S.; Masic, A.; Prajatelista, E.; Iordachescu, M.; Waite, J.H. Marine hydroid perisarc: A chitin- and melanin-reinforced composite with DOPA-iron (III) complexes. *Acta Biomater.* **2013**, *9*, 8110-8117.
118. Knight, D.P. Sclerotization of the perisarc of the calyptoblastic hydroid, *Laomedea flexuosa*. 2. Histochemical demonstration of phenol oxidase and attempted demonstration of peroxidase. *Tissue Cell* **1971**, *3*, 57-64.
119. Miserez, A.; Rubin, D.J.; Waite, J.H. Crosslinking chemistry of squid beak. *J. Biol. Chem.* **2010**, *285*, 38115-38124.
121. Narkar, A.R.; Cannon, E.; Yildirim-Alicea, H.; Ahn, K. Catechol-functionalized chitosan: optimized preparation method and its interaction with mucin. *Langmuir* **2019**, *35*, 16013-16023.
122. Kim, E.; Liu, Z.; Liu, Y.; Bentley, W.E.; Payne, G.F. Catechol-based hydrogel for chemical information processing. *Biomimetic* **2017**, *2*, 11.
123. Miserez, A.; Liu, Y.; Waite, J.H. Jumbo squid beaks: inspiration for design of robust organic composites. *Acta Biomaterialia* **2007**, *3*, 139-149.
124. Oh, D.X.; Hwang, D.S. A biomimetic chitosan composite with improved mechanical properties in wet conditions. *Biotechnol. Prog.* **2013**, *29*, 505-512.
127. Zhang, X.; Hassanzadeh, P.; Miyake, T.; Jin, J.; Rolandi, M. Squid beak inspired water processable chitosan composites with tunable mechanical properties. *J. Mater. Chem. B* **2016**, *4*, 2273-2279.
128. Zhou, M.; Liu, Q.; Wu, S.; Gou, Z.; Wu, X.; Xu, D. Starch/chitosan films reinforced with polydopamine modified MMT: effects of dopamine concentration. *Food Hydrocolloids* **2016**, *61*, 678-684.
129. Zvarec, O.; Purushotham, S.; Masic, A.; Ramanujan, R.V.; Miserez, A. Catechol-functionalized chitosan/iron oxide nanoparticle composite inspired by mussel thread coating and squid beak interfacial chemistry. *Langmuir* **2013**, *29*, 10899-10906.
130. Nor, S.S.; Samer, H.H.; Aminu, K.; Mohd, Z.H.; Sharida, F.; Abdul, H.S. Synthesis and characterization of magnetic chitosan-L-dopa nanocomposites. *Current Nanoscience* **2016**, *12*, 487-492.
131. Bae, K.H.; Park, M.; Do, M.J.; Lee, N.; Ryu, J.H.; Kim, G.W. Chitosan oligosaccharide-stabilized ferromagnetic iron oxide nanocubes in magnetically modulated cancer hyperthermia. *ACS Nano* **2012**, *6*, 5266-5273.
132. Ni, K.; Zhou, X.; Zhao, L.; Wang, H.; Ren, Y.; Wei, D. Magnetic catechol-chitosan with bioinspired adhesive surface: preparation and immobilization of transaminase. *PLoS One* **2017**, *7*, e41101.
133. Jiang, P.L.; Hou, R.Q.; Chen, C.D.; Sun, L.; Dong, S.G.; Pan, J.S.; Lin, C.J. Controllable degradation of medical magnesium by electrodeposited composite films of mussel adhesive protein and chitosan. *J. Colloid Interface Sci.* **2016**, *478*, 246-255.
134. Lee, K.; Oh, M.H.; Lee, M.S.; Nam, Y.S.; Park, T.G.; Jeong, J.H. Stabilized calcium-phosphate nano-aggregates using a dopamine-chitosan conjugate for gene delivery. *Int. J. Pharmaceutics* **2013**, *445*, 196-202.

135. Cao, X.; Hou, D.; Wang, L.; Li, S.; Sun, S.; Ping, Q.; Xu, Y. Effects and molecular mechanism of chitosan-coated levodopa nanoliposomes on behavior of dyskinesia rats. *Biol Res* **2016**, *49*, 32 (9p).
136. Qiao, H.; Sun, M.; Su, Z.; Xie, Y.; Chen, M.; Zong, L. Kidney-specific drug delivery system for renal fibrosis based on coordination-driven assembly of catechol-derived chitosan. *Biomaterials* **2014**, *35*, 7157-7171.
137. Sakono, N.; Nakamura, K.; Ohshima, T.; Hayakawa, R.; Sakono, M. Tyrosinase-mediated peptide conjugation with chitosan-coated gold nanoparticles. *Analyt. Sci.* **2019**, *35*, 79-83.
138. Amato, A.; Migneco, L.M.; Martinelli, A.; Pietrelli, L.; Piozzi, A.; Francolini, I. Antimicrobial activity of catechol-functionalized chitosan versus *Staphylococcus epidermis*. *Carbohydr. Polym.* **2018**, *179*, 273-281.
139. Cu, T.S.; Cao, V.D.; Nguyen, C.K.; Tran, N.Q. Preparation of silver core-chitosan shell nanoparticles using catechol-functionalized chitosan and antibacterial studies. *Macromol. Res.* **2014**, *22*, 418-423.
140. Vale, A.C.; Pereira, P.; Barbosa, A.M.; Torrado, E.; Mano, J.F.; Alves, N.M. Antibacterial free-standing polysaccharide composite films inspired by the sea. *Int. J. Biol. Macromolec.* **2019**, *133*, 933-944.
141. Almeida, A.C.; Vale, A.C.; Pires, R.A.; Reis, R.L.; Alves, N.M. Layer-by-layer films based on catechol-modified polysaccharides produced by dip- and spin-coating onto different substrates. *J. Biomed. Mater. Res.* **2019**, 1-6.
142. Moreira, J.; Vale, A.C.; Pires, R.A.; Botelho, G.; Reis, R.L.; Alves, N.M. Spin-coated polysaccharide-based multi-layered freestanding films with adhesive and bioactive moieties. *Molecules* **2020**, *25*, 840.
143. Huang, W.; Bao, X.; Liu, Y.; Wang, Z.; Hu, Q. Catechol-functional chitosan/silver nanoparticle composite as a highly effective antibacterial agent with species-specific mechanisms. *Sci. Reports* **2017**, *7*, 1860.
144. Wang, Y.; Zhu, L.; You, J.; Chen, F.; Zong, L.; Yan, W.; Li, C. Catecholic coating and silver hybridization of chitin nanocrystals for ultrafiltration membranes with continuous flow catalysis and gold recovery. *ACS Sust. Chem. Eng.* **2017**, *5*, 10673-10681.
145. Ryu, J.H.; Hong, S.; Lee, H. Bio-inspired adhesive catechol-conjugated chitosan for biomedical applications. *Acta Biomater.* **2015**, *27*, 101-115.
146. Xu, J.; Soliman, G.M.; Barralet, J.; Cerruti, M. Mollusk glue inspired mucoadhesives for biomedical applications. *Langmuir* **2012**, *28*, 14010-14017.
147. Ryu, J.H.; Jo, S.; Koh, M.H.; Lee, H. Bio-inspired, water-soluble to insoluble self-conversion for flexible, biocompatible, transparent, catecholamine polysaccharide thin films. *Adv. Funct. Mater.* **2014**, *24*, 7709-7716.
148. Kim, E.; Liu, Y.; Shi, X.W.; Yang, X.; Bentley, W.E.; Payne, G.F. Biomimetic approach to confer redox activity to thin chitosan films. *Adv. Funct. Mater.* **2010**, *20*, 2683-2694.
149. Oh, D.X.; Hwang, D.S. A biomimetic chitosan composite with improved mechanical properties in wet conditions. *Biotechnol. Prog.* **2013**, *29*, 505-512.
150. Lee, J.M.; Ryu, J.H.; Kim, E.A.; Jo, S.; Kim, B.S.; Lee, H. Adhesive barrier/directional controlled release for cartilage repair by endogenous progenitor cell recruitment. *Biomaterials* **2015**, *39*, 173-181.
151. Ruprai, H.; Shanu, A.; Mawad, D.; Hook, J.M.; Kilian, K.; George, L.; Wuhner, R.; Houang, J.; Myers, S.; Lauto, A. Porous chitosan adhesives with L-DOPA for enhanced photochemical tissue bonding. *Acta Biomaterialia* **2020**, *101*, 314-326.

152. Xu, Y.; Liang, K.; Ullah, W.; Ji, Y.; Ma, J. Chitin nanocrystal enhanced wet adhesion performance of mussel-inspired citrate-based soft-tissue adhesive. *Carbohydr. Polym.* **2018**, *190*, 324-330.
153. Soliman, G.M.; Zang, Y.L.; Merle, G.; Cerruti, M.; Barralet, J. Hydrocaffeic acid-chitosan nanoparticles with enhanced stability, muco-adhesion and permeation properties. *Eur. J. Biopharm.* **2014**, *88*, 1026-1037.
154. Kim, K.; Ryu, J.H.; Lee, D.Y.; Lee, H. Bio-inspired catechol conjugation converts water-insoluble chitosan into a highly water-soluble adhesive chitosan derivative for hydrogels and LbL assembly. *Biomaterials Sci.* **2013**, *1*, 783-790.
155. Xu, J.; Strandman, S.; Zhu, J.X.X.; Barralet, J.; Cerruti, M. Genipin-crosslinked catechol-chitosan mucoadhesive hydrogels for buccal drug delivery. *Biomaterials* **2015**, *37*, 395-404.
156. Peng, X.; Peng, Y.; Han, B.; Liu, W.; Zhang, F.; Linhardt, R.J. IO₄⁻ stimulated crosslinking of catechol-conjugated hydroxyethyl chitosan as a tissue adhesive. *J. Biomed. Mater. Res. B* **2019**, *107*, 582-593.
157. Byun, E.; Ryu, J.H.; Lee, H. Catalyst-mediated yet catalyst-free hydrogels formed by interfacial chemical activation. *Chem. Commun.* **2014**, *50*, 2869-2872.
158. Krogsgaard, M.; Hansen, M.R.; Birkedal, H. Metals and polymers in the mix: fine-tuning the mechanical properties and color of self-healing mussel-inspired hydrogels. *J. Mater. Chem. B* **2014**, *2*, 8292-8297.
159. Yavvari, P.S.; Srivastava, A. Robust self-healing hydrogels synthesized from catechol-rich polymers. *J. Mater. Chem. B* **2015**, *3*, 899-910.
160. Jing, X.; Mi, H.Y.; Napiwocki, B.N.; Peng, X.F.; Turng, L.S. Mussel-inspired electroactive chitosan/graphene oxide composite hydrogel with rapid self-healing and recovery behaviour for tissue engineering. *Carbon* **2017**, *125*, 557-570.
161. Andersen, A.; Krogsgaard, M.; Birkedal, H. Mussel-inspired self-healing double-cross-linked hydrogels by controlled combination of metal coordination and covalent linking. *Biomacromolec.* **2018**, *19*, 1402-1409.
162. Ryu, J.H.; Lee, Y.; Kong, W.H. Catechol-functionalized chitosan/pluronic hydrogels for tissue adhesives and hemostatic materials. *Biomacromolec.* **2011**, *12*, 2653-2659.
163. Zhang, D.Y.; Hu, Z.; Lu, S.T.; Li, S.D.; Yang, Z.M.; Li, P.W. Preparation and characterization of catechol-functionalized chitosan thermosensitive hydrogels. *IOP Conf. Series Mater Sci Eng.* **2019**, *629*, 012038.
164. Kim, E.; Liu, Z.; Liu, Y.; Bentley, W.E.; Payne, G.F. Catechol-based hydrogel for chemical information processing. *Biomimetic* **2017**, *2*, 11.
165. Cholewonski, A.; Yang, F.; Zhao, B. Algae-mussel inspired hydrogel composite glue for underwater bonding. *Mater. Horizons* **2019**, *6*, 285-293.
166. Pandey, N.; Hakamivala, A.; Xu, C.; Haribaran, P.; Rodioniv, B.; Huang, Z.; Liao, J.; Tang, L.; Zimmern, P.; Nguyen, K.T.; Hong, Y. Biodegradable nanoparticles enhanced adhesiveness of mussel-like hydrogels at tissue interface. *Adv Healthcare Mater* **2018**, *7*, 1701069.
167. Lee, C.; Shin, J.; Lee, J.S.; Bruyn, E.; Ryu, J.H.; Um, S.H.; Kim, D.I.; Lee, H.; Cho, S.W. Bioinspired calcium free alginate hydrogels with tunable physical and mechanical properties and improved biocompatibility. *Biomacromolecules* **2013**, *14*, 2004-2013.
168. Lee, Y.K.; Lee, S.Y. A colorimetric alginate-catechol hydrogel suitable as a spreadable pH indicator. *Dyes Pigments* **2014**, *108*, 1-6.
169. Kondaveeti, S.; Cornejo, D.R.; Petri, D.F. Alginate/magnetite hybrid beads for magnetically stimulated release of dopamine. *Coll. Surf. B* **2016**, *138*, 94-101.

170. Alegre-Requena, J.V.; Haring, M.; Herrera, R.P.; Diaz, D.D. Regulatory parameters of self-healing alginate hydrogel networks prepared via mussel-inspired dynamic chemistry. *NJC* **2016**, *40*, 8493-8501.
171. Yan, S.; Wang, W.; Li, X.; Ren, J.; Yun, W.; Zhang, K.; Li, G.; Yin, J. Preparation of mussel-inspired injectable hydrogels based on dual-functionalized alginate with improved adhesive, self-healing and mechanical properties. *J. Mater. Chem. B* **2018**, *6*, 6377-6390.
172. Scognamiglio, F.; Travan, A.; Borgogna, M.; Donati, L.; Marsich, E.; Bosmans, J.W.; Perge, L.; Foulc, M.P.; Bouvy, N.D.; Paoletti, S. Enhanced bioadhesivity of dopamine-functionalized polysaccharidic membranes for general surgery applications. *Acta Biomater.* **2016**, *44*, 232-242.
173. Donati, I.; Draget, K.I.; Borgogna, M.; Paoletti, S.; Skjak-Braek, G. Tailor-made alginate bearing galactose moieties on mannuronic residues. *Biomacromolec.* **2005**, *6*, 88-98.
174. Ponzio, F.; Le Houerou, V.; Zafeiratos, S.; Gauthier, C.; Garnier, T.; Jierry, L.; Ball, V. Robust alginate-catechol polydopamine free-standing membranes obtained from the air/water interface. *Langmuir* **2017**, *33*, 2420-2426.
175. Korytowski, W.; Sarna, T.; Kalyanaraman, B.; Sealy, R.C. Tyrosinase-catalyzed oxidation of dopa and related catechol(amine)s: a kinetic electron spin resonance investigation using spin-stabilization and spin label oximetry. *Biochim. Biophys. Acta* **1987**, *924*, 383-392.
176. Fu, J.; Li, D.; Li, G.; Huang, F.; Wei, Q. Carboxymethyl cellulose assisted immobilization of silver nanoparticles onto cellulose nanofibers for the detection of catechol. *J. Electroanal. Chem.* **2015**, *738*, 92-99.
177. Fu, J.; Pang, Z.; Yang, J.; Huang, F.; Cai, Y.; Wei, Q. Fabrication of polyaniline/carboxymethyl cellulose/cellulose nanofibrous mats and their biosensing applications. *Appl. Surf. Sci.* **2015**, *349*, 35-42.
178. Fan, H.; Wang, J.; Zhang, Q.; Jin, Z. Tannic acid-based multifunctional hydrogels with facile adjustable adhesion and cohesion contributed by polyphenol supramolecular chemistry. *ACS Omega* **2017**, *2*, 6668-6676.
179. Yang, B.; Lim, C.; Hwang, D.S.; Cha, H.J. Switch of surface adhesion to cohesion by Dopa-Fe³⁺ complexation, in response to microenvironment at the mussel plaque/substrate interface. *Chem. Mater.* **2016**, *28*, 7982-7989.
180. Yu, J.; Wei, W.; Danner, E.; Ashley, R.K.; Israelachvili, J.; Waite, J.H. Mussel protein adhesion depends on interprotein thiol-mediated redox modulation. *Nat. Chem. Biol.* **2011**, *7*, 588-590.
181. Fan, H.; Wang, L.; Feng, X.; Bu, Y.; Wu, D.; Jin, Z. Supramolecular hydrogel formation based on tannic acid. *Macromolecules* **2017**, *50*, 666-676.
182. Sun, C.; Xiong, B.; Pan, Y.; Cui, H. Adsorption removal of tannic acid from aqueous solution by polyaniline: analysis of operating parameters and mechanism. *J. Colloid Interface Sci.* **2017**, *487*, 175-181.
183. Guo, J.; Sun, W.; Kim, J.P.; Lu, X.; Li, Q.; Lin, M.; Mrowczynski, O.; Rozk, E.B.; Cheng, J.; Qian, G.; Yang, J. Development of tannin-based bioadhesives. *Acta Biomater.* **2018**, *72*, 35-44.
184. Hu, Z.; Cranston, E.D.; Ng, R.; Pelton, R. Tuning cellulose nanocrystal gelation with polysaccharides and surfactants. *Langmuir* **2014**, *30*, 2684-2692.
185. Tang, H.R.; Covington, A.D.; Hancock, R.A. Structure-activity relationships in the hydrophobic interactions of polyphenols with cellulose and collagen. *Biopolymers* **2003**, *70*, 403-413.
186. Bu, Y.; Zhang, S.; Cai, Y.; Yang, Y.; Ma, S.; Huang, J.; Xu, W. Fabrication of durable antibacterial and superhydrophobic textiles via in situ synthesis of silver nanoparticle on tannic-acid coated viscose textiles. *Cellulose* **2019**, *3*, 2109-2122.
187. Hanif, Z.; Khan, Z.A.; Siddiqui, M.F.; Tariq, M.Z.; Park, S.; Park, S.J. Tannic acid-mediated rapid layer-by-layer deposited non-leaching silver nanoparticles hybridized cellulose membranes for point-of-use-water disinfection. *Carbohydr. Polym.* **2020**, *231*, 115746.

188. Huang, J.; Cheng, Y.; Wu, Y.; Shi, X.; Du, Y.; Dang, H. Chitosan/tannic acid gillayers layer-by-layer deposited cellulose nanofibrous mats for antimicrobial application. *Int. J. Biol. Macromol.* **2019**, *139*, 191-198.
189. Hu, Z.; Berry, R.M.; Pelton, R.; Cranston, E.D. One-pot water-based hydrophobic surface modification of cellulose nanocrystals using plant polyphenols. *ACS Sus. Chem. Eng.* **2017**, *5*, 5018-5026.
190. Foo, M.L.; Tan, C.R.; Lim, P.D.; Ooi, C.W.; Tan, K.W.; Chew, I.M. Surface-modified nanocrystalline cellulose from oil palm empty fruit bunch for effective binding of curcumin. *Int. J. Biol. Macromol.* **2019**, *138*, 1064-1071.
191. Rubentheren, V.; Ward, T.A.; Chee, C.Y.; Nair, P.; Salami, E.; Fearday, C. Effects of heat treatment on chitosan nanocomposite film reinforce with nanocrystalline cellulose and tannic acid. *Carbohydr. Polym.* **2016**, *140*, 202-208.
192. Wang, Z.; Mo, L.; Zhao, S.; Li, J.; Zhang, S.; Huang, A. Mechanically robust nacre-mimetic framework constructed polypyrrole-doped graphene/nanofiber nanocomposites with improved thermal electrical properties. *Mater. Design* **2018**, *155*, 278-287.
193. Wang, Z.; Kang, H.; Zhao, S.; Zhang, W.; Zhang, S.; Li, J. Polyphenol-induced cellulose nanofibrils anchored graphene oxide as nanohybrids for strong yet tough soy protein nanocomposites. *Carbohydr. Polym.* **2018**, *180*, 354-364.
194. Ge, W.; Cao, S.; Shen, F.; Wang, Y.; Ren, J.; Wang, X. Rapid self-healing, stretchable, moldable, antioxidant and antibacterial tannic acid-cellulose nanofibril composite hydrogel. *Carbohydr. Polym.* **2019**, *224*, 115147.
195. Ji, Y.; Wen, Y.; Wang, Z.; Zhang, S.; Guo, M. Eco-friendly fabrication of a cost-effective cellulose nanofiber-based aerogel for multifunctional applications in Cu(II) and organic pollutants removal. *J. Clean. Prod.* **2020**, *255*, 120276.
196. Zhang, Z.Y.; Sun, Y.; Zheng, Y.D.; He, W.; Yang, Y.Y.; Xie, Y.J.; Feng, Z.X.; Qiao, K. A biocompatible bacterial cellulose/tannic acid composite with antibacterial and anti-biofilm activities for biomedical applications. *Mater. Sci. Eng. C* **2020**, *106*, 110249.
197. Hong, S.; Yang, K.; Kang, B.; Lee, C.; Song, I.T.; Byun, E. Hyaluronic acid catechol: a biopolymer exhibiting a pH-dependent adhesive or cohesive property for human neural stem cell engineering. *Adv. Funct. Mater.* **2013**, *23*, 1774-1780.
198. Lee, Y.; Lee, H.; Kim, Y.B.; Kim, J.; Hyeon, T.; Park, H. Bioinspired surface immobilization of hyaluronic acid on monodisperse magnetite nanocrystals for targeted cancer imaging. *Adv. Mater.* **2008**, *20*, 4154-4157.
199. Kim, K.; Ryu, J.H.; Lee, D.Y.; Lee, H. Bio-inspired catechol conjugation converts water-insoluble chitosan into highly water-soluble, adhesive chitosan derivatives for hydrogels and LbL assembly. *Biomater. Sci.* **2013**, *1*, 426-430.
200. Kim, K.; Kim, K.; Ryu, J.H.; Lee, H. Chitosan-catechol: a polymer with long-lasting mucoadhesive properties. *Biomaterials* **2015**, *52*, 161-170.
201. Lee, D.; Park, J.P.; Koh, M.Y.; Kim, P.; Lee, J.; Shin, M.; Lee, H. Chitosan-catechol: a writable bioink under serum culture media. *Biomater. Sci.* **2018**, *6*, 1040-1047.
202. Sobolewski, P.; Goszczynska, A.; Aleksandrak, M.; Urbas, K.; Derkowka, J.; Bartoszewska, A.; Podolski, J.; Mijowska, E.; El Fray, M. A biofunctionalizable ink platform composed of catechol-modified chitosan and reduced graphene oxide/platinum nanocomposite. *Beilstein J. Nanotechnol.* **2017**, *8*, 1508-1514.
203. Elegir, G.; Kindl, A.; Sadocco, P.; Orlandi, M. Development of antimicrobial cellulose packaging through laccase-mediated grafting of phenolic compounds. *Enzyme Microbial Technol.* **2008**, *43*, 84-92.

204. Sun, X.; Bai, R.; Zhang, Y.; Wang, Q.; Fan, X.; Yuan, J.; Cui, L.; Wang, P. Laccase-catalyzed oxidative polymerization of phenolic compounds. *Appl. Biochem. Biotechnol.* **2013**, 171, 1673-1680.
205. Kim, S.Y.; Zille, A.; Murkovic, M.; Guebitz, G.; Cavaco-Paulo, A. Enzymatic polymerization on the surface of functionalized cellulose fibers. *Enzyme Microb. Technol.* **2007**, 40, 1782-1787.
206. Zhai, R.; Chen, X.; Jin, M.; Hu, J. Synthesis of a polydopamine nanoparticle/bacterial cellulose composite for use as a biocompatible matrix for laccase immobilization. *Cellulose* **2019**, 26, 8337-8349.
207. Sampaio, L.M.; Padrao, J.; Faria, J.; Silva, J.P.; Silva, C.J.; Dourado, F.; Zille, A. Laccase immobilization on bacterial nanocellulose membranes: Antimicrobial, kinetic and stability properties. *Carbohydr. Polym.* **2016**, 145, 1-12.
208. Song, J.E.; Su, J.; Noro, J.; Cavaco-Paulo, A.; Silva, C.; Kim, H.R. Bio-coloration of bacterial cellulose assisted by immobilized laccase. *AMB Express* **2018**, 8, 19.
209. Su, J.; Noro, J.; Fu, J.; Wang, Q.; Silva, C. Enzymatic polymerization of catechol under high-pressure homogenization for the green coloration of textiles. *J. Clean. Prod.* **2018**, 202, 792-798.